CCM-80-8

Center for Composite Materials

DIGITAL ANALYSIS OF ULTRASONIC WAVES IN COMPOSITES

ROBERT A. BLAKE, JR.

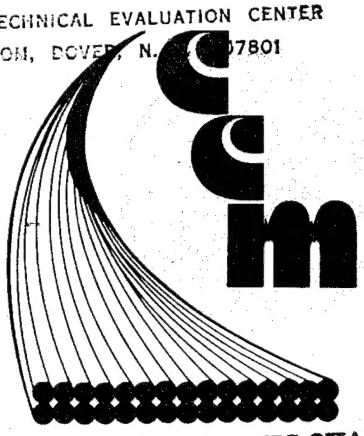

College of Engineering
University of Delaware
Newark, Delaware

*MSG DI4 DROLS PROCESSING - LAST INPUT IGNORED

*MSG DI4 DROLS PROCESSING-LAST INPUT IGNORED

*MSG DI4 DROLS PROCESSING - LAST INPUT IGNORED

--   1 OF   1
--   ***DTIC DOES NOT HAVE THIS ITEM***
-- 1 - AD NUMBER: D430430
-- 5 - CORPORATE AUTHOR: DELAWARE UNIV NEWARK CENTER FOR COMPOSITE
--   MATERIALS
-- 6 - UNCLASSIFIED TITLE: DIGITAL ANALYSIS OF ULTRASONIC WAVES IN
--   COMPOSITES.
-- 9 - DESCRIPTIVE NOTE: 31 JAN 77 - 8 OCT 79,
--10 - PERSONAL AUTHORS: BLAKE,R. A. , JR.;
--11 - REPORT DATE: MAY   , 1980
--12 - PAGINATION: 86P
--14 - REPORT NUMBER: CCM-80-8
--20 - REPORT CLASSIFICATION: UNCLASSIFIED
--22 - LIMITATIONS (ALPHA):   APPROVED FOR PUBLIC RELEASE; DISTRIBUTION
--   UNLIMITED. AVAILABILITY: CENTER FOR COMPOSITE MATERIALS, UNIVERSITY
--   OF DELAWARE, NEWARK, DE. 19711.
--33 - LIMITATION CODES: 1 24

--END   << ENTER NEXT COMMAND >>   END --

DIGITAL ANALYSIS OF

ULTRASONIC WAVES IN COMPOSITES

BY

Robert Alvin Blake, Jr.

A thesis submitted to the faculty of the University of Delaware in partial fulfillment of the requirements for the degree of Master of Electrical Engineering.

May 1980

Center for Composite Materials
University of Delaware
Newark, Delaware 19711

FOREWARD

The work reported herein was sponsored by the Center for Composite Materials, University of Delaware, Newark, Delaware. The work was performed during the period from January 31, 1977 to October 8, 1979. The principal investigators were Robert A. Blake, Jr., and Dr. R. Byron Pipes.

The author would like to thank Dr. L. P. Bolgiano, Dr. J. P. Allebach and Dr. W. R. Scott for their guidance and assistance throughout the program.

TABLE OF CONTENTS

LIST OF FIGURES

(List of Figures, continued)

ABSTRACT

The methodology to nondestructively evaluate, both qualitatively and quantitatively, the characteristics and properties of composite materials is explored. The methods are based on amplitude measurements and frequency decomposition of ultrasonic waveforms. The development of the facility and the selection of digital equipment rather than analog is discussed. The signal processing capabilities and the nondestructive inspection abilities of the facility are covered in detail. Determination of material properties by ultrasonic measurements is performed in the frequency domain and comparisons are made with mechanical test data. The benefits of frequency domain measurements over time domain measurements are discussed. Examples of ultrasonic C-scans are given for oriented fiber composites. Characterization of delaminated structures is explored in detail along with the effect of delaminations on both the time and frequency representations of the ultrasonic waveform.

I. INTRODUCTION

The ultrasonic inspection and evaluation of fiber-reinforced composite materials has proven to be a valuable tool in the characterization of material defects and in the determination of fiber orientation and measurement of material properties. The ability to know something about the condition of a material before it is tested in a mechanical testing apparatus is very important if one is interested in valid measurement of material elastic constants. The determination of flow patterns in short fiber injection molded composites by ultrasonic C-scan techniques has explained failure modes in these specimens. In addition to qualitative ultrasonic nondestructive inspection of composite materials, the quantitative evaluation of material elastic constants by nonmechanical methods is very useful. Using ultrasonic measurement it is possible to evaluate material properties which are very difficult or impossible to measure using a mechanical testing apparatus. These measurements are necessary for determining a complete matrix of material constants from which the behavior of the material under various conditions of stress can be determined.

The objective of the research recorded in this report was to develop a facility for the nondestructive evaluation of composite materials and to develop the signal processing capabilities necessary for the analysis and application of ultrasonic waveforms toward the measurement of material properties. The tools required to meet this objective are discussed in detail in the chapters which follow. The most important tool needed in any system is flexibility. It is for this reason that it was decided to develop a facility which was capable of digital signal processing rather than investing in analog signal processing devices. In an analog system any change or modification requires changes in hardware which incur higher costs in both time and money. A digital system can be programmed to perform many tasks and, as system requirements change, a digital system can be reprogrammed to handle different types of data and display the results in a variety of forms. The digital system does not lock the user into a specific type of analysis and is therefore a more flexible and valuable research tool than its analog counterpart.

The types of measurements which needed to be made were primarily amplitudes and delays. Except in the performing of a basic C-scan, it is not clear exactly how or where to take measurements in the time domain representation

of the ultrasonic waveform. It is, however, very clear what measurements need to be taken in the frequency domain and the method of taking the measurements is accurate and valid over a specified range. It was therefore decided, with respect to material property determination, that frequency domain measurements be given priority. All of the signal processing techniques developed in this report were validated through comparison with known or experimental data.

Chapter II discusses the nondestructive testing facility and describes each of the electronic components of the system. The function and capabilities of each component are discussed. The discussion is separated into two parts. The first section describes an ultrasonic C-scan system. A C-scan is a X-ray image of the internal characteristics of a material. The image is formed using sound waves rather than X-rays and the image is formed on conductive paper instead of film. The C-scan is formed by scanning the material one line at a time. This differs from the full field view of a X-ray image. Despite these differences, X-ray images and C-scan images appear similar and each has its advantages and disadvantages. This report uses C-scans when displaying the internal structure of a material. The second section of Chapter II describes the signal processing components of the system and discusses the various methods

of displaying the ultrasonic information.

Chapter III discusses information necessary for the analysis of ultrasonic waveforms in the frequency domain. The fast Fourier transform is discussed and the effects of waveform quantization and sampling duration are investigated.

Chapter IV applies the techniques of Chapter III to perform measurements of source spectrums, thicknesses and velocities of sound. The use of spectral division and phase angle computations are necessary in the above measurements.

Chapter V concludes with a statement which summarizes the benefits of digital and frequency domain measurement techniques.

II. ULTRASONIC NONDESTRUCTIVE TESTING FACILITY

2.1 Ultrasonic C-Scan System

The formation of an ultrasonic C-scan requires the use of at least four devices which can possibly be combined into one or more pieces of equipment. It is necessary to couple the ultrasonic transducer to the specimen and also to scan the specimen with the transducer in the x-y plane of the specimen. It is also desirable to obtain a digital output of the transducer's x and y coordinates. The scanning device must be linked to a display device either mechanically or electrically via the x and y coordinate output. The display device is normally one of two types. A CRT display is capable of displaying information based upon a threshold setting. If the input information is above a set threshold, the display point on the CRT is illuminated; otherwise it remains dark. A conductive paper display allows the amplitude of the incoming signal to be represented as a shade of gray and also produces a permanent record of the image without the need of photography or a separate hard copy device. The piece of equipment purchased to perform the above tasks was a TekTran ultrasonic immersion recording

scanner model SR-254. This unit, shown in Figure 1, incorporates both the scanning device and display device into one unit. It displays the output C-scan on conductive paper which yields a 1:1 image of the specimen. The transducer location is displayed on two four-digit digital displays which indicate the x and y coordinates to 0.001 inch.

The ultrasonic analyzer is the most important device in an ultrasonic C-scan system. It must be capable of sending high voltage pulses with a high repetition rate to the ultrasonic transducer and then receive the reflected or transmitted waveform through the same or a second receiver transducer. It must be able to select all or part of the received waveform for analysis and the selected or gated portion must be triggerable from both the initial pulse and the first reflection. The unit must also display the waveform or send the signal and a trigger pulse to an oscilloscope. It is also beneficial to send both the total and gated portions of the waveform to the oscilloscope for comparison. The unit which was purchased to meet the above specifications was a Panametrics model 5052UA selected for its high repetition rate of 5,000 Hz and because it incorporates the pulser, receiver, stepless gate and gated peak detector into one unit. The unit does not contain a waveform display but it is capable of sending the waveform to

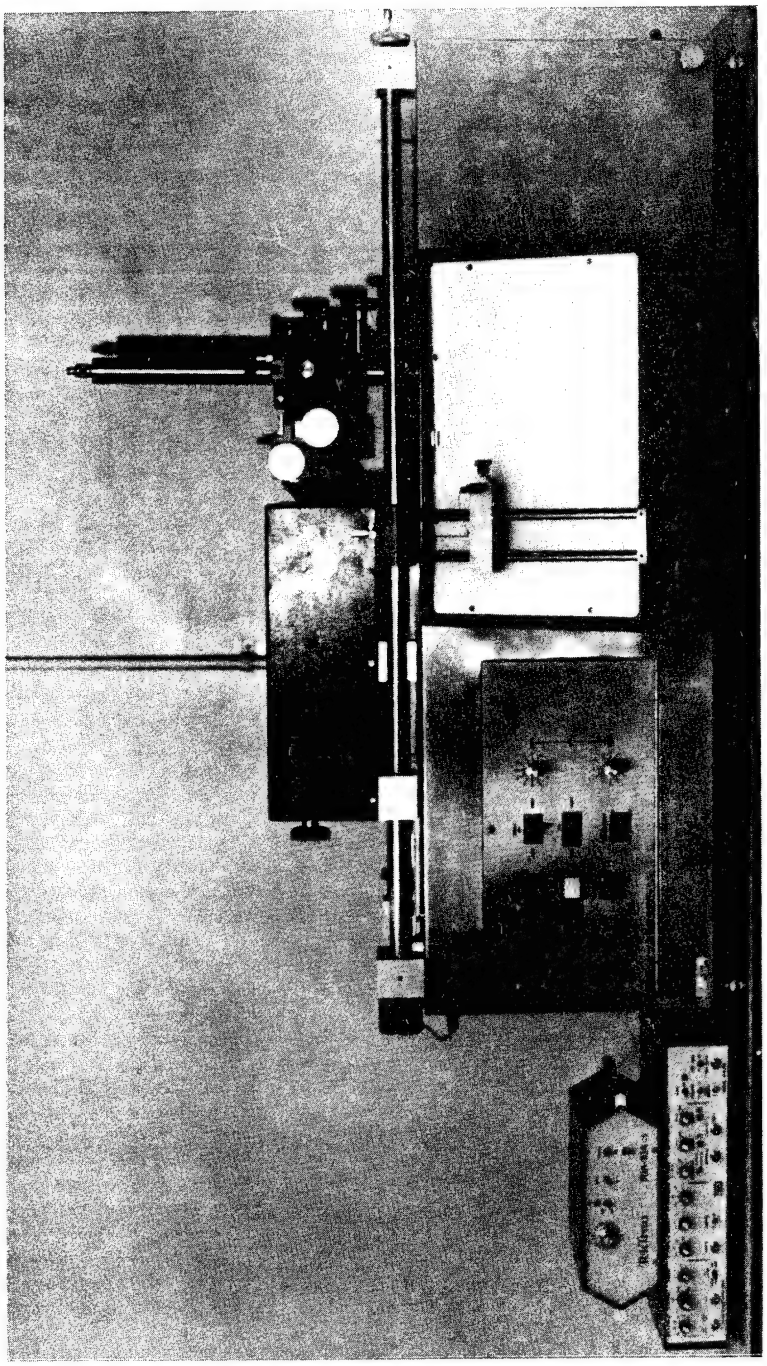

Figure 1. Ultrasonic Immersion Scanner

an oscilloscope which has a delayed trigger mode. The oscilloscope used to monitor the waveform is a Tektronix model 565 dual-beam oscilloscope. Both the total and gated waveforms can be displayed simultaneously on this unit.

The fourth device necessary to form a C-scan is either an amplifier or a threshold detector. A threshold detector is normally used with a CRT display to produce a signal when the amplitude of the ultrasonic waveform is above a set threshold. This type of a device is not capable of gray scale image production. The image formed on the CRT display represents information which is either above or below one threshold value. The CRT display is turned on only when the threshold value is exceeded and a point is plotted on the CRT which corresponds to a specific point on the sample. The final image is composed of only white and black areas. The amplifier used in the present system is composed of ten preset thresholds, each of which corresponds to a different shade of gray. In this device, when the input signal exceeds a given threshold, a discrete increase in current is transmitted to the "hot pen" which contacts the surface of the conductive paper and forms a dot with a shade of gray corresponding to the amplitude of the ultrasonic waveform at that point on the specimen. The amplifier purchased for this purpose was a TekTran model RIA-10A TS,

shown in Figure 2 along with the Panametrics ultrasonic analyzer. The amplifier is also capable of accepting a BCD encoded digital signal to specify the shade of gray displayed on the immersion scanner. Thus, digital computer control of the amplifier and the image is possible.

The final device was designed and constructed for ease of operation and set-up of controls. It is a gray scale indicator and is shown in Figure 3. This device has two modes of operation, allowing either a bar or dot display to indicate the shade of gray at a point on the C-scan. The device is composed of ten analog comparators whose threshold voltages are set in ascending one-volt increments. The output of each comparator illuminates a light-emitting diode (LED) on the display. An audible alarm is activated if the input voltage exceeds the highest shade of gray, thus indicating saturation of the pen amplifier. This type of digital LED display was desired rather than an analog meter because of its fast response to rapidly changing signals.

The system just described allows the user to form A-scans and C-scans which give information concerning the quality of the material being examined. The A-scan is the time representation of the waveform and is shown in Figure 4 with the following abbreviations:

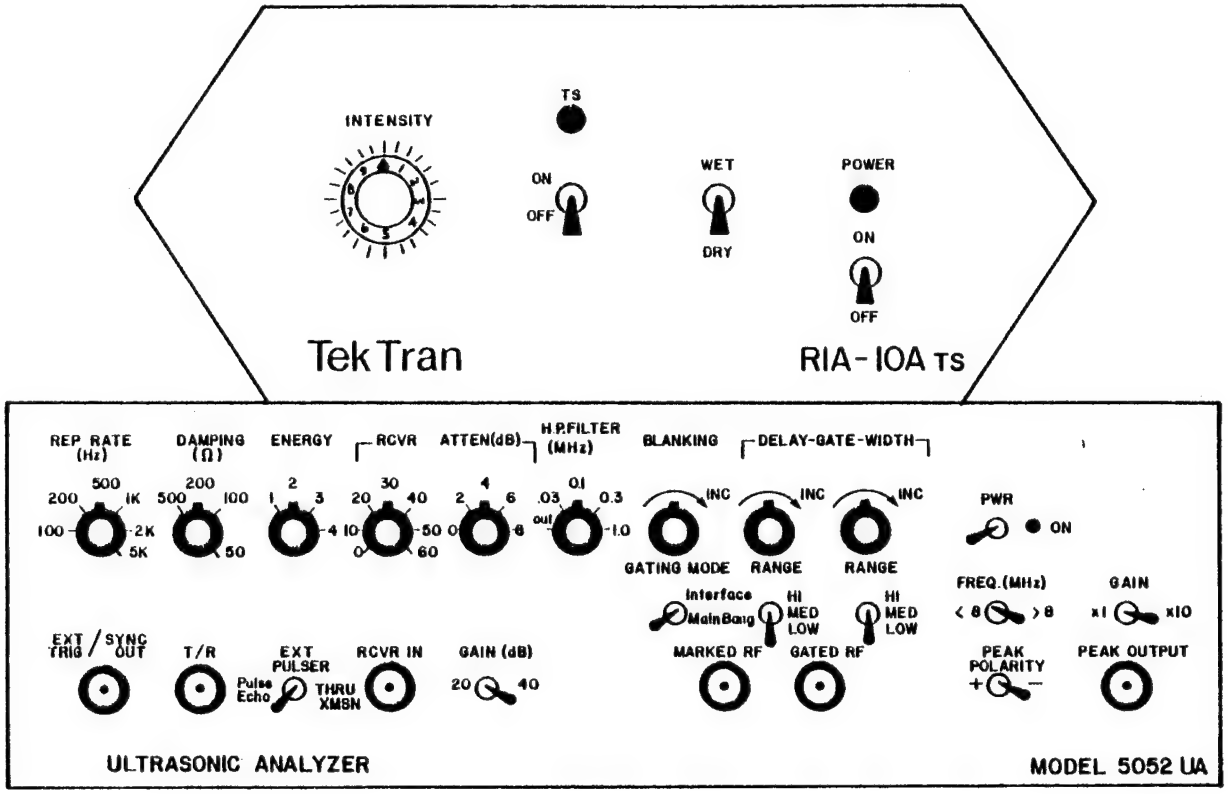

Figure 2. Ultrasonic Analyzer and Pen Amplifier

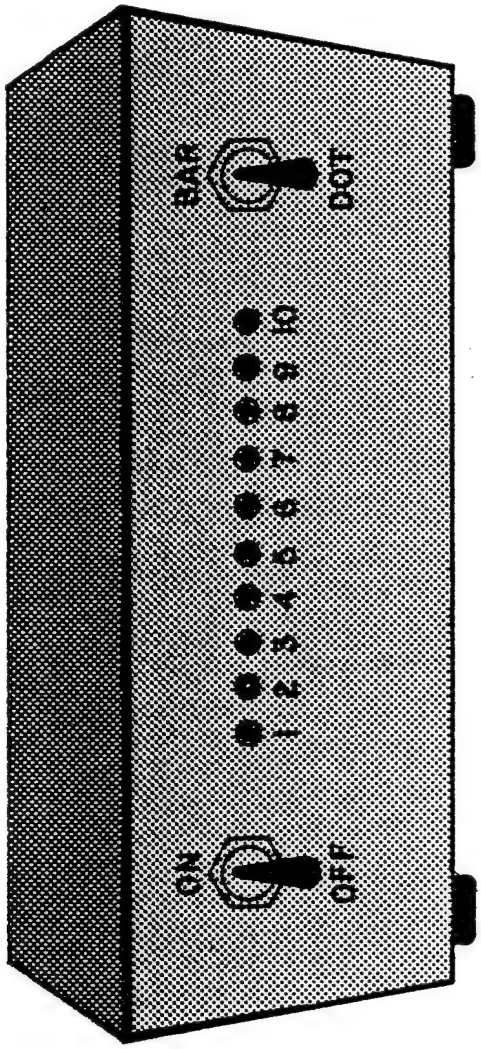

Figure 3. Gray Scale Indicator

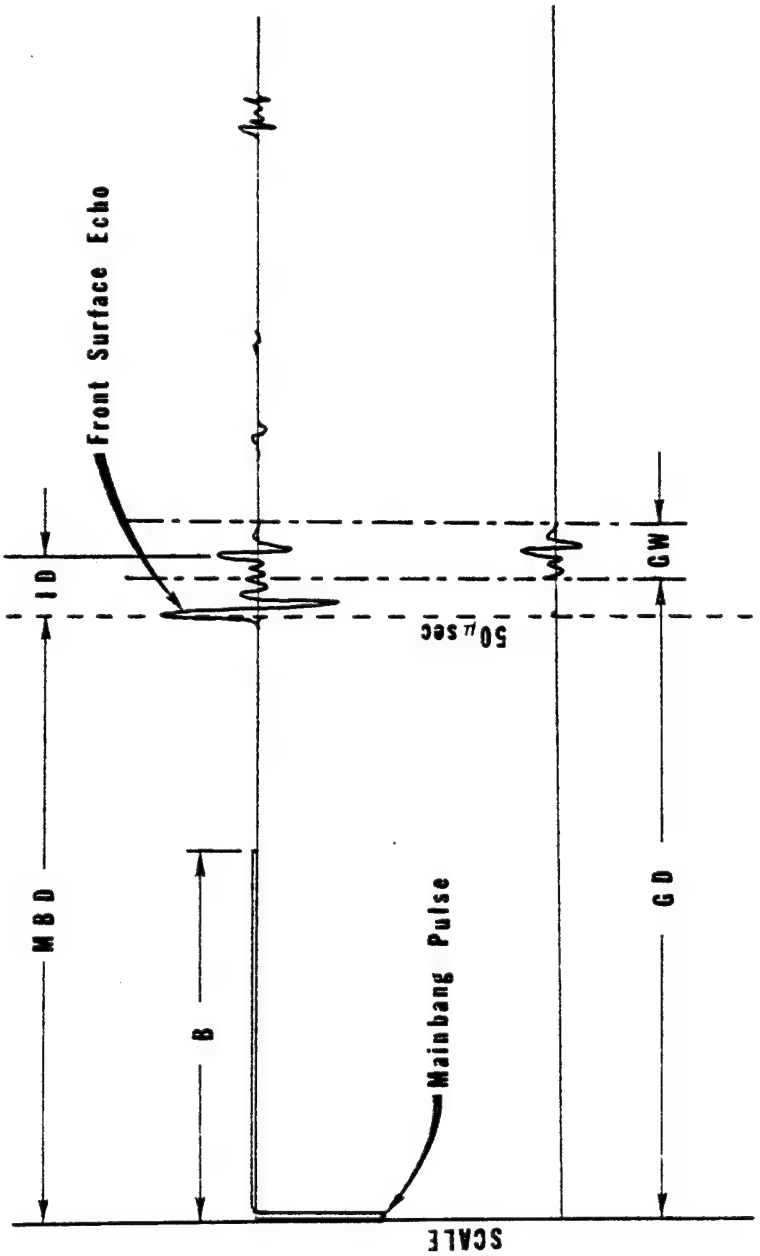

Figure 4. A-Scan Waveform Schematic

- MBD is the main bang delay, which is the time between the initial main bang pulse and the front surface echo of the specimen. This time is dependent on the focal length of the transducer and is set to 50 microseconds for all scans included in this report.

- ID is the interface delay, which is the time between the front surface echo and the back surface echo. This delay is dependent on the thickness of the sample and the speed of sound in a given material.

- GD and GW are the gate delay and the gate width, respectively. They are recorded in order to accurately reproduce scans at a later date.

- B is the blanking distance. This can be used in situations when it is desirable to trigger the gate from a surface other than the front surface of the sample.

An ultrasonic C-scan can be formed by using all or part of the information contained in a family of A-scans. In the ultrasonic pulse-echo technique, a wide band pulse

approximately one microsecond in duration is emitted by a tuned and focused transducer (Figure 5). The waves reflected from the specimen front and back surfaces are received by the transmitting transducer. The received waveform is conditioned by gating circuitry in a manner which allows a selected portion of the total waveform to be analyzed; the selected portion of the total waveform is then termed the gated waveform (Figure 6). The gated waveform is analyzed in a peak detector circuit which identifies the amplitude of the largest peak within the gated waveform. The polarity of the peak is user-selectable; therefore, the positive and negative portions of the gated waveform may be investigated independently. The amplitude of the largest peak is converted into a square pulse of corresponding amplitude which can then be amplified if necessary to drive the recorder pen amplifier. In the pen amplifier, the amplitude of the square pulse is quantized into ten regions ranging from 0 to 10 volts in one-volt increments. Each region corresponds to a different shade of gray on the C-scan with ten volts being the darkest region. A corresponding quantized D.C. voltage is then sent to current-limiting circuitry which controls the input to the hot pen recorder. The voltage at the pen tip remains constant and the current is varied so that different amounts

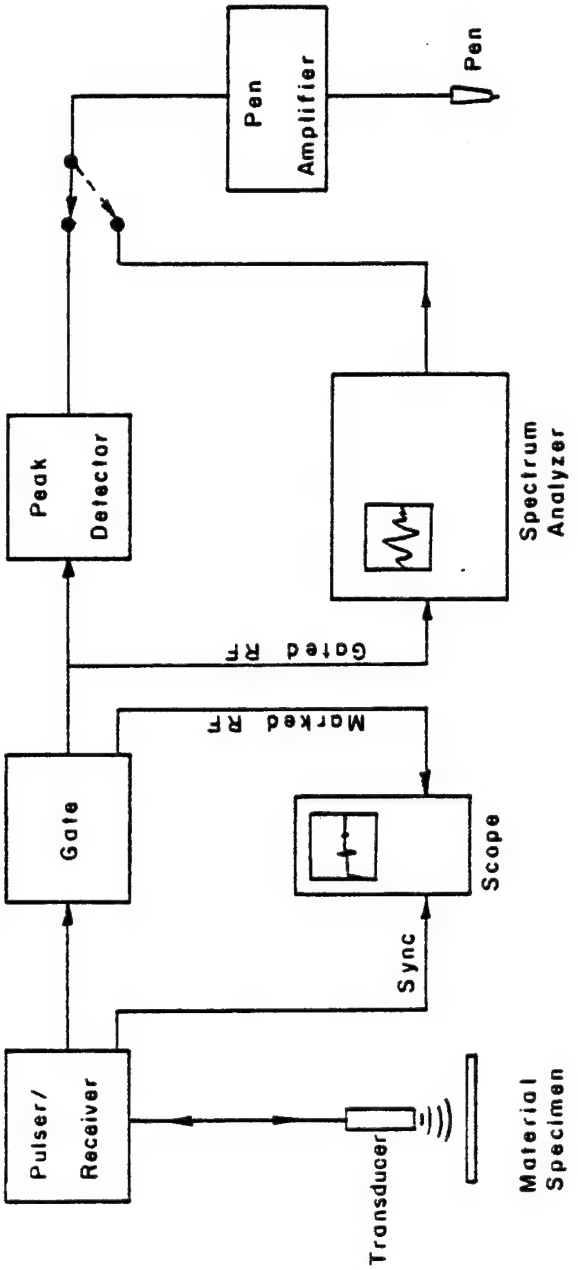

Figure 5. Block Diagram of Ultrasonic System

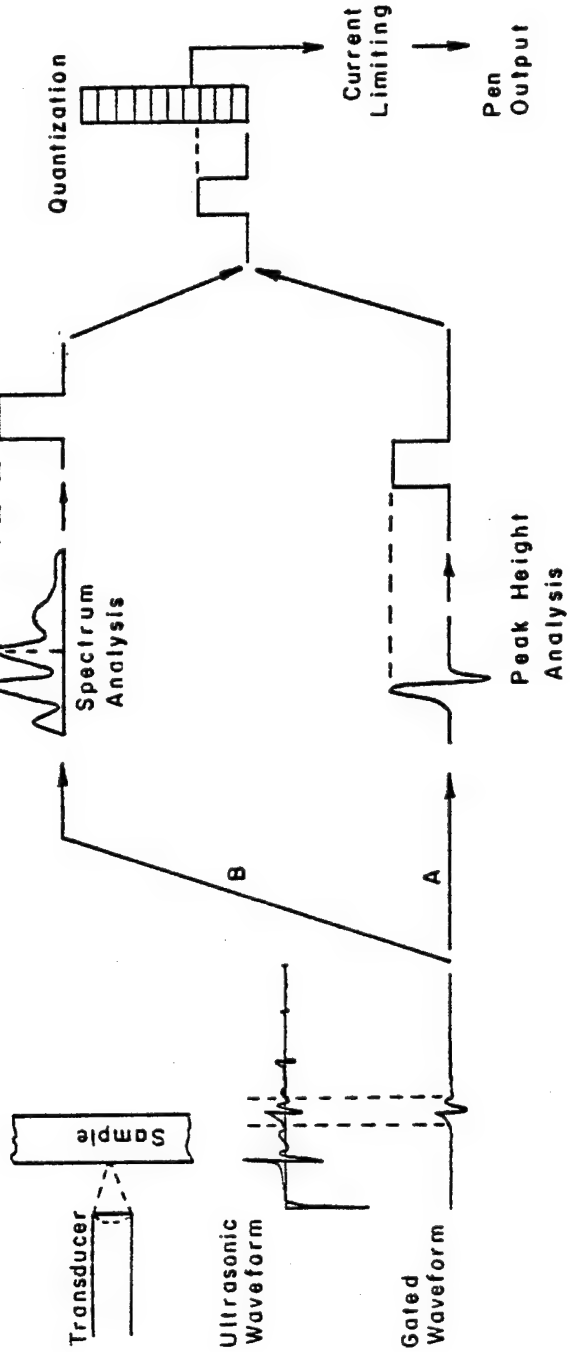

Figure 6. Waveform Gating and Quantization

of oxide are burned off of the ink-impregnated, oxide-coated paper. The image is formed by scan lines composed of dots whose shade of gray corresponds to the amplitude of the gated waveform at that point on the specimen (Figure 7). The scan lines are normally spaced at 0.010 inch horizontally, and the number of dots per inch vertically is between 200 and 500 depending on the scan speed. Decreasing the horizontal spacing below 0.010 inch does little to improve the image since the pen tip diameter is 0.012 inch.

2.2 Ultrasonic Signal Processing System

Any system which is designed to perform digital signal processing can be separated into three groups of components. Herein these three groups will be labeled: input/output (I/O) components; data processing components; and, data sampling and digitizing components. The signal processing facility developed for the analysis of ultrasonic waveforms is diagrammed in Figure 8. The system's I/O components are a DEC LA36 paper teminal, a Tektronix CRT graphic display terminal, a paper tape reader/punch, and an Omnitec telephone modem. These components are all directly connected to either the parallel or serial interface ports of a Digital LSI II minicomputer which was expanded by an additional sixteen dual card slots in a Digital expansion unit.

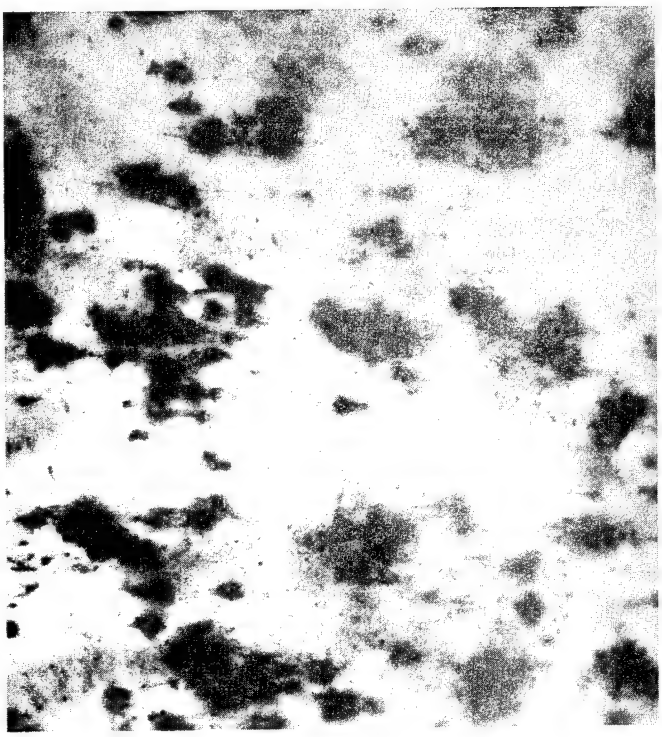

X100

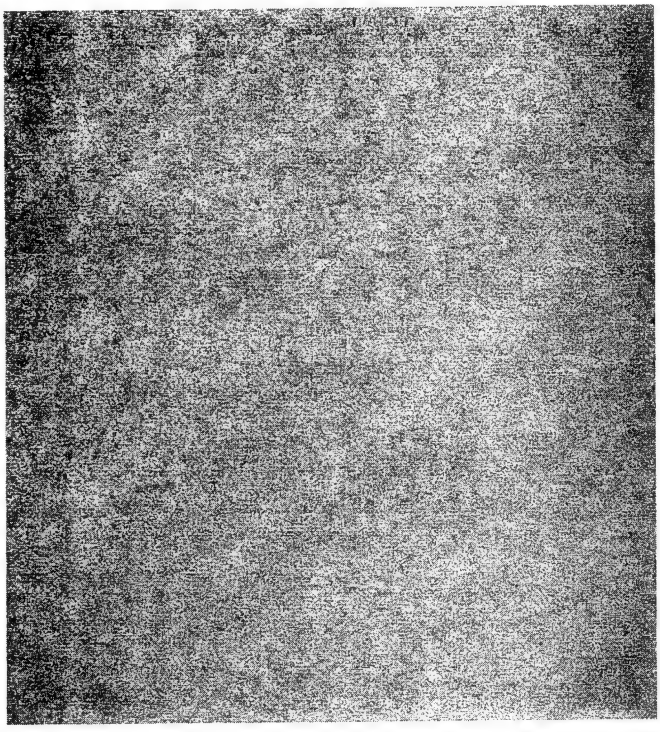

X1

Figure 7. C-Scan Image Composition

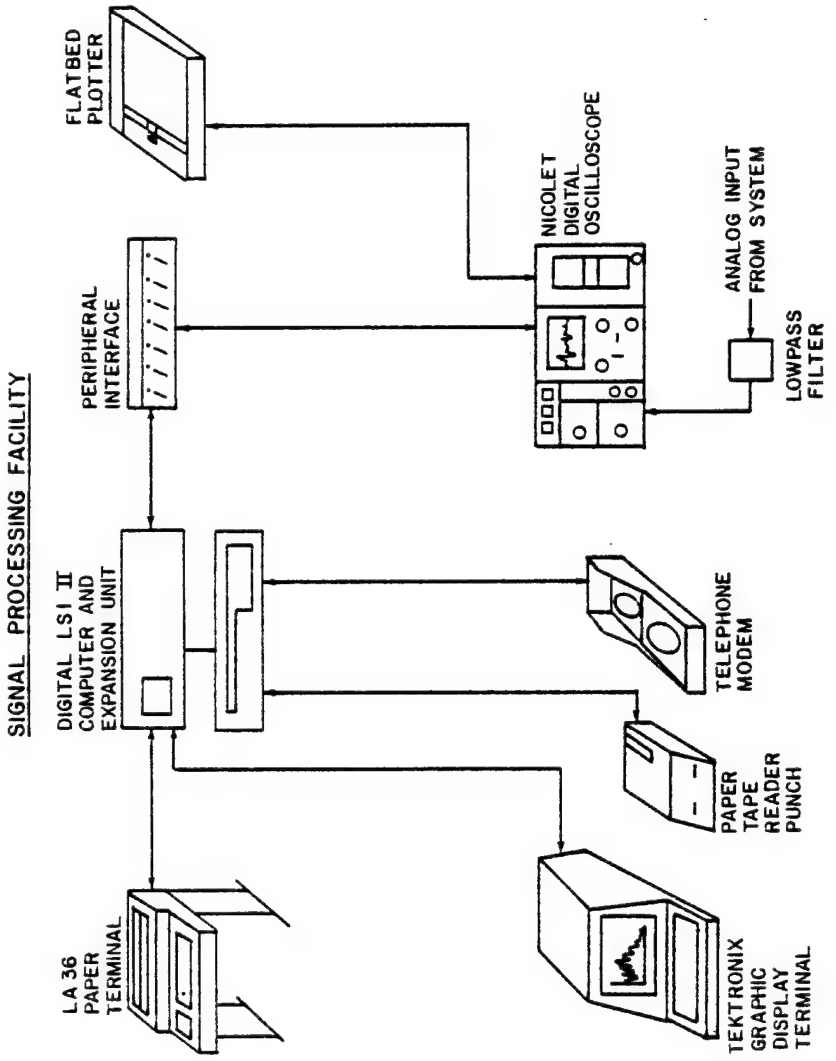

Figure 8. Signal Processing Facility

The LA36 terminal is used as the main control terminal and is used to control all data input and output, and data transfers between the LSI II and the telephone modem which is connected to a Burroughs B7700 computer. The LA36 also is used to output ultrasonic data in tabular form and to print program listings. A small degree of graphic output is also possible on the LA36; however, the resolution is limited to the printer's character and line spacing. Therefore, whenever graphic output is desired, control is transferred from the LA36 to the Tektronix graphic terminal.

The data sampling and digitizing component in the system is a Nicolet digital oscilloscope. The oscilloscope has a miximum sampling rate of 20 MHz and digitizes the input to eight bits. The oscilloscope has the ability to store waveforms on a self-contained floppy disk and can also output waveforms to a flatbed plotter. Since the maximum frequency which can be digitized on this unit without aliasing is 10 MHz, a 10-MHz low pass filter, whose 3 dB point is at 10 MHz and which is 65 dB down at 11 MHz, is used to pre-filter all inputs. A peripheral interface was constructed to join the Nicolet oscilloscope to the LSI II computer. The interface expands 16 input bits and 25 output bits on the LSI II to 112 input bits and 112 output bits.

The oscilloscope requires 25 input bits and 20 output bits for control and data input and ouput. The remaining bits of the interface will be used for system expansion. All output bits are tristate controlled from the front panel of the peripheral interface. This allows data and control lines to be set in the proper states prior to data transmissions and also allows manual operation of the oscilloscope. In order to perform the required data transmissions and manipulations, a control program named NICDAT was written in LSI II machine language. The details of the program are flow charted in Appendix A along with the control characters used to run the program. The program allows control of the paper tape reader and transfer of control between the Tektronix terminal and the LA36 terminal. The program also transmits a break signal upon the receipt of a "Control B" command. This is necessary because the break key halts the program execution and transfers control to the LSI II monitor. The primary use of the program is to control the peripheral interface connected to the Nicolet digital oscilloscope. This function of the program allows the transmission of data between set limits from the oscilloscope to an external computer where the data can be stored and analyzed.

With the addition of the digital oscilloscope to the

ultrasonic C-scan system, it is possible to form amplitude plots and digital A-scans. The formation of an amplitude plot requires plotting the amplitude information from the gated waveform in an x-y coordinate plane. The spacing of the scan lines is 0.25 inch. The amplitude plot formation results in a three-dimensional image of the materials internal structure. The resolution is a function of the plot spacing in the y direction and the interrogation rate in the x direction. It is, therefore, possible for 0.25-inch diameter defects to be undetected in this example. The measure of the resolution is somewhat better than this when the probability of a 0.25-inch defect occurring exactly between the scan lines is considered. The waveform shown in the center of Figure 9 was formed by monitoring the amplitude from the gated peak detector as the sample was transversed at a constant velocity. The noise present in the waveform was due to the sampling rate of the digitizer, as well as the interrogation rate of the pulser. The signal from the gated peak detector ramps from zero volts to the output value for the remainder of the pulse. The noise occurs when the digitizer samples the output before it reaches its peak value. The noisy signal was then filtered to remove the signal portion of the waveform and the D.C. bias was removed. This is the waveform shown at the bottom

ultrasonic C-scan system, it is possible to form amplitude plots and digital A-scans. The formation of an amplitude plot requires plotting the amplitude information from the gated waveform in an x-y coordinate plane. The spacing of the scan lines is 0.25 inch. The amplitude plot formation results in a three-dimensional image of the materials internal structure. The resolution is a function of the plot spacing in the y direction and the interrogation rate in the x direction. It is, therefore, possible for 0.25-inch diameter defects to be undetected in this example. The measure of the resolution is somewhat better than this when the probability of a 0.25-inch defect occurring exactly between the scan lines is considered. The waveform shown in the center of Figure 9 was formed by monitoring the amplitude from the gated peak detector as the sample was transversed at a constant velocity. The noise present in the waveform was due to the sampling rate of the digitizer, as well as the interrogation rate of the pulser. The signal from the gated peak detector ramps from zero volts to the output value for the remainder of the pulse. The noise occurs when the digitizer samples the output before it reaches its peak value. The noisy signal was then filtered to remove the signal portion of the waveform and the D.C. bias was removed. This is the waveform shown at the bottom

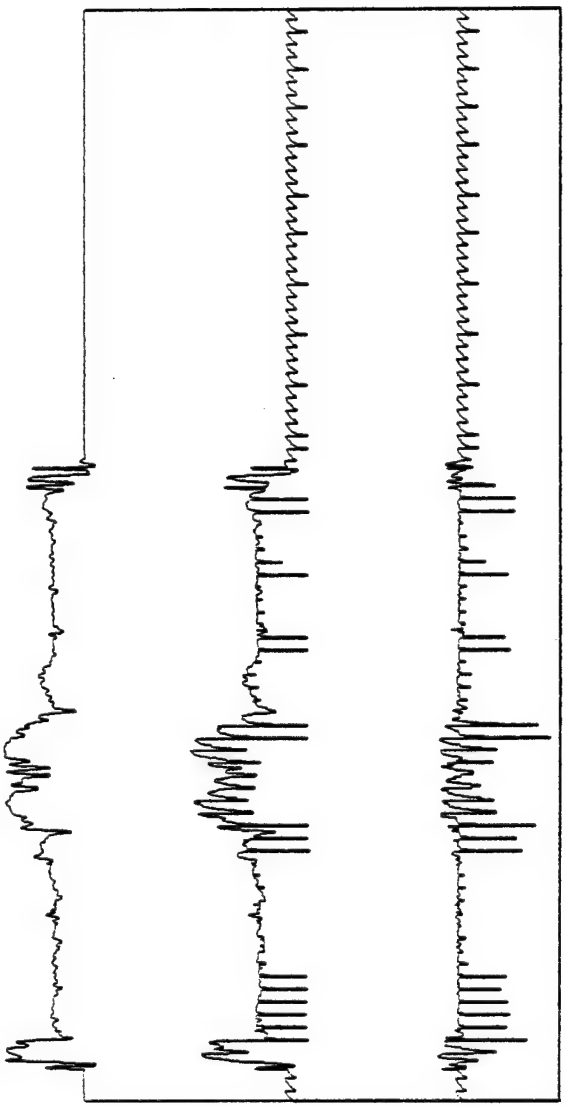

Figure 9. Amplitude Plot Formation

of Figure 9 and is called the noise waveform. The noise waveform is then subtracted from the signal-plus-noise waveform in a differential amplifier yielding the signal waveform shown at the top of Figure 9. If the waveform is filtered in an attempt to remove the noise directly, the waveform becomes less detailed or some noise remains.

A C-scan of half of a circular disk with a circular defect in the center is shown in Figure 10. An amplitude plot of this disk is shown in Figure 11. The amplitude plot accurately shows the delaminated center section, as well as the delaminated edge region. The amplitude plot, however, does not yield information about fine structure such as fiber orientation, whereas the C-scan does.

An image of a plane perpendicular to the material can be formed from a family of A-scans spaced at equal intervals. A C-scan of one half of a circular disk containing a circular delamination and a delaminated circumference is shown in Figure 12. A line has been drawn across a region containing a delamination. A-scans were taken at points marked on the line. The family of A-scans representing this line is shown in Figure 13. This A-scan was formed by sampling the waveform with a digital oscilloscope. The oscilloscope time base was set for a spacing of 50 nsec

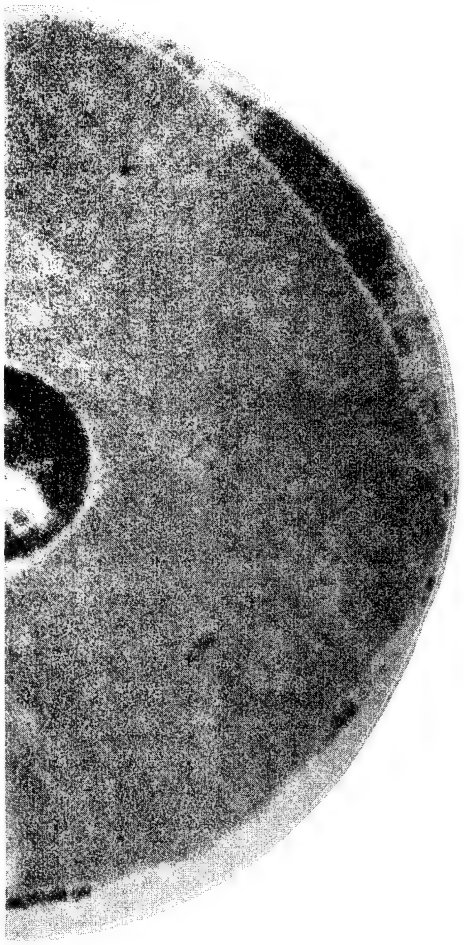

Figure 10. C-Scan of Half Disk

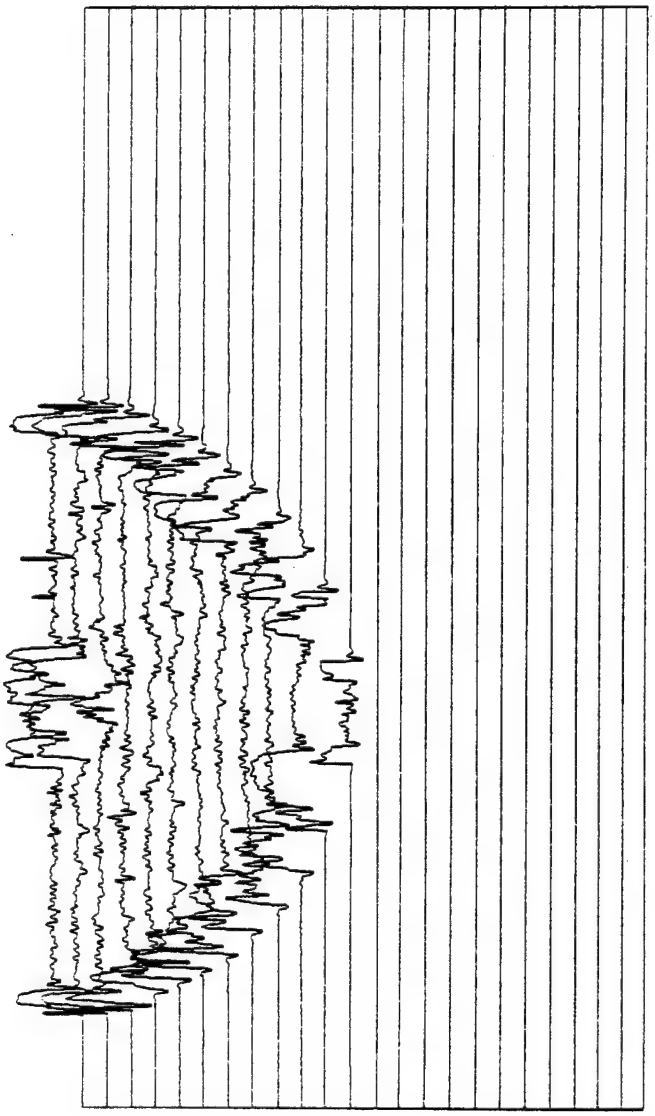

Figure 11. Amplitude Plot of Half Disk

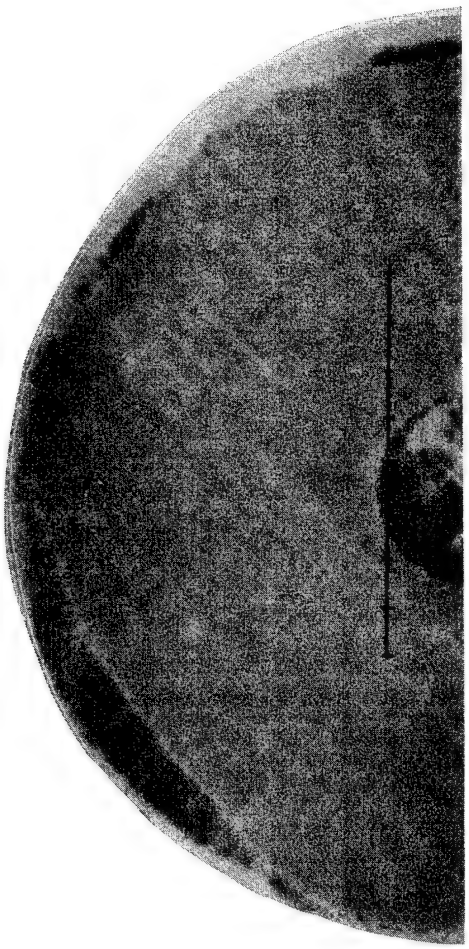

Figure 12. C-Scan of Half Disk with Line

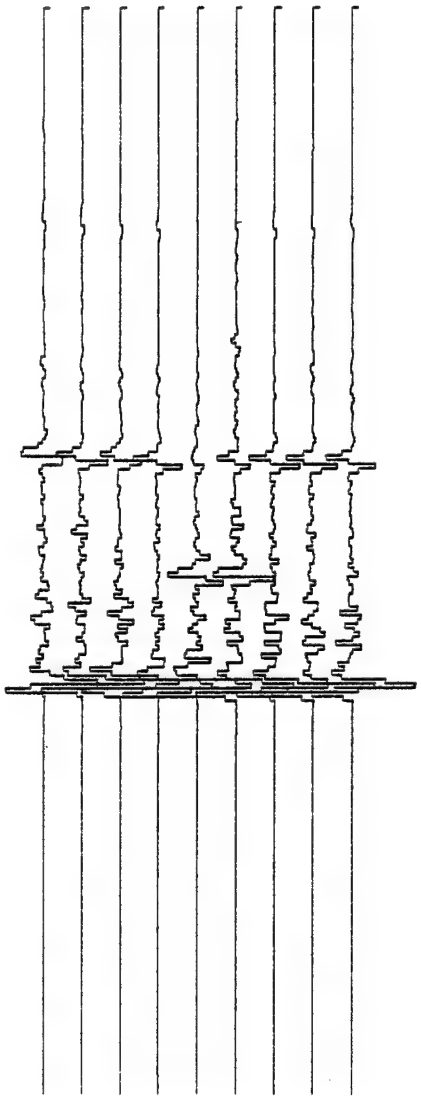

Figure 13. A-Scan of Disk

between sample points. The data was then plotted with straight lines connecting the points. The data could be further analyzed using a digital computer to interpolate between the data points. This interpolation could be accompolished by using either a polynomial curve-fit algorithm or by taking the Fourier transform of the data and then forming a reconstruction of the waveform, evaluated at smaller spacings than was present in the initial data. The adjusted data could then be displayed on the oscilloscope or plotted to form a family of A-scans which reveal improved smoothness.

The effectiveness of an interpolation technique which incorporates a fast Fourier transform will now be demonstrated (the fast Fourier transform will be discussed in detail in the next chapter). Figure 14 shows a waveform from a 64-ply graphite-epoxy sample which had a Teflon defect implanted between its center plies. The waveform was sampled at 50 ηsec/pt and was plotted without straight lines between the sample points. The data from this waveform was Fourier transformed and eight zeros were added for each point in the original frequency spectrum. An inverse Fourier transform was performed on the adjusted set of data and the result is plotted in Figure 15. The interpolation which was performed in the frequency domain

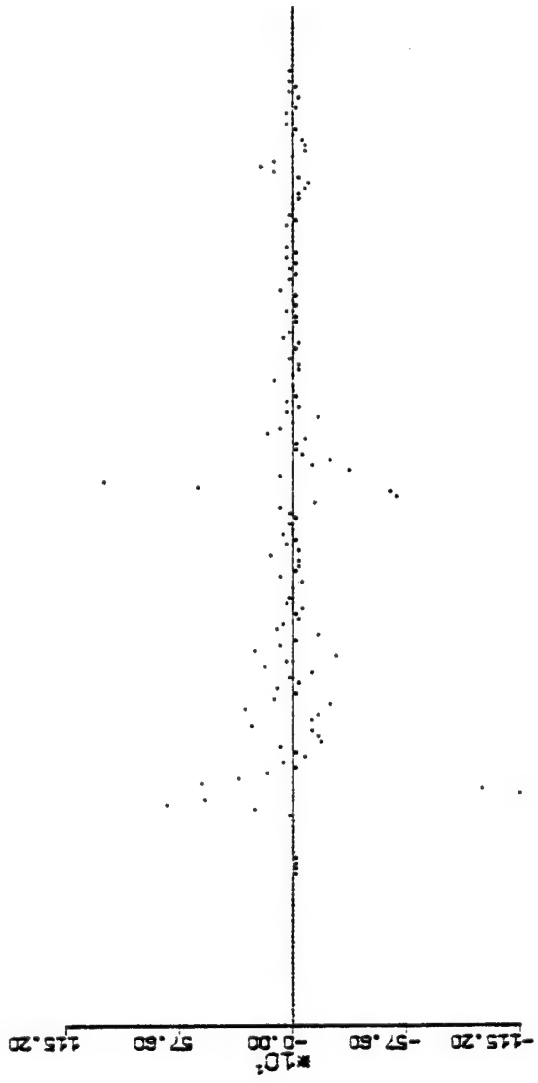

Figure 14. 64-Ply Graphite Center Defect Sampled at 50 ηsec/pt

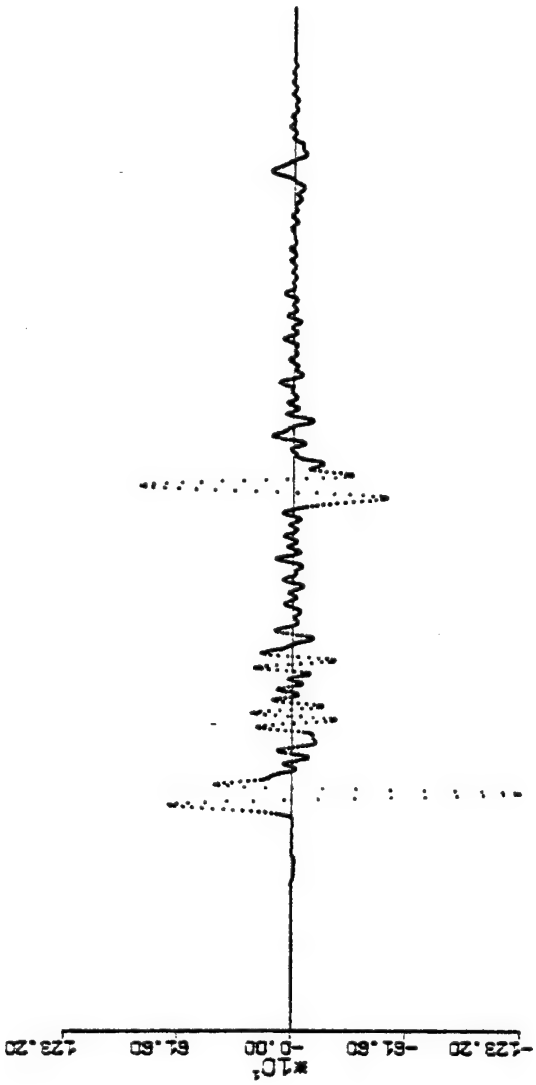

Figure 15. 64-Ply Graphite Center Defect Interpolated to 6.25 nsec/pt

yields a time domain waveform with eight times as many points than were originally present.

The computer analysis of a family of A-scans can be used to produce B-scans giving information related to positions of defects, through the thickness. The B-scan can be made of either the amplitude or time information of the A-scan to form two types of B-scans. A B-scan using amplitude information produces an image which resembles a C-scan except that the image is of a plane perpendicular to the sample rather than in the plane of the sample. This concept is shown in Figure 16. The amplitude of a point on the A-scan waveform is converted into a gray scale point on the B-scan in the same manner as the C-scan. This results in an image which has a dark line corresponding to the front surface echo and a lighter line corresponding to the back surface echo. The shades of gray of the front surface line and the back surface line correspond to the amplitude of the front surface echo and the back surface echo, respectively. Any delamination will appear as a dark gray region on the B-scan. If delaminations at various depths are present, as shown in Waveform C of Figure 16, the back surface echo becomes attenuated and thus the shade of gray of the back surface line becomes white. It should be noted that this technique can show multiple stacked

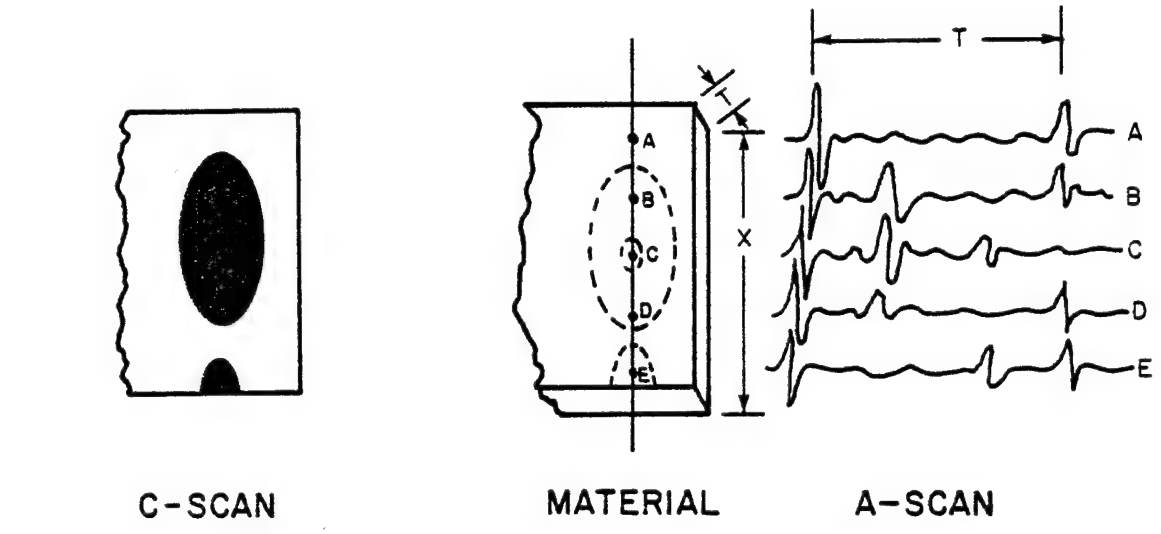

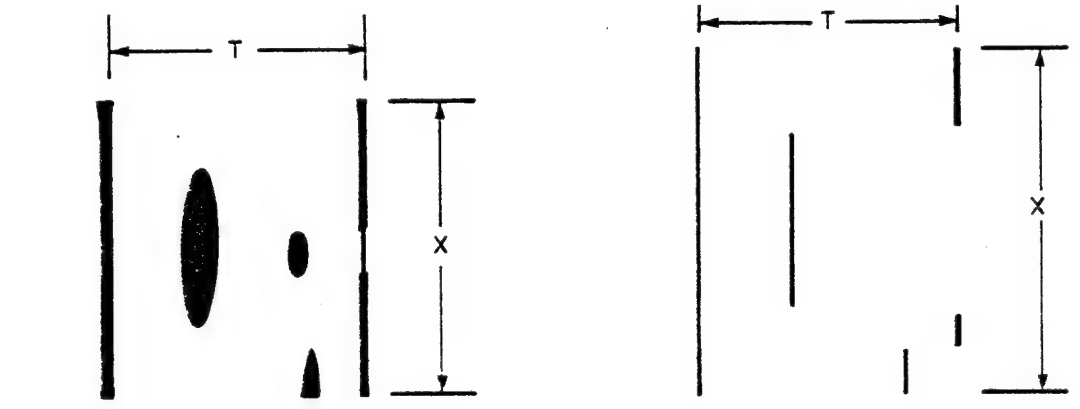

Figure 16. B-Scan Formation

delaminations, but care must be taken in interpreting the image beyond the first delamination because it is possible for second multiple reflections from large delaminations to appear as "false" delaminations spaced at regular intervals. The spacing of the false delaminations will correspond to the distance between the front surface and the first delamination.

A B-scan using time information is also shown in Figure 16. This scan is composed of lines which indicate the amount of time between the front surface echo and the first echo which exceeds a set threshold. This threshold can also be a function of time which depends on the attenuation of the ultrasonic wave. A decaying exponential is an example of such a function. This type of B-scan will only show the first delamination present. All lines are the same thickness and no gray scale is involved. This eliminates the problem of multiple reflections but all structural detail is lost by using this simple representation. Computer-aided techniques can be used for the time-based B-scan to form a three-dimensional image of the defect planes. This image can be easily displayed by a graphic computer terminal.

III. PROBLEMS INVOLVED IN IMPLEMENTING SPECTRAL COMPUTATIONS

3.1 Fast Fourier Transform (FFT)

The frequency spectrum of an ultrasonic waveform may be obtained by using an analog spectrum analyzer; however, an analog spectrum analyzer is a very specialized component in an ultrasonic system and is limited in the number of operations it can perform as well as in the form of data presented. A more versatile approach to forming the frequency spectrum of an ultrasonic waveform is by digitally sampling the waveform at a rate greater than twice the highest frequency component in the wavefore and then evaluating the discrete Fourier transform of the sample points.[1] The Fourier transform of a time-dependent function $f(t)$ is $F(j\omega)$ and is defined in equation 3.1 .

$$F(j\omega) = \int_{-\infty}^{\infty} f(t)e^{-j\omega t}\,dt \qquad (3.1)$$

---

[1]Stearns. Digital Signal Analysis, New Jersey, Hayden, 1975.

The discrete Fourier transform (DFT), $\overline{F}(j\omega)$, is defined as the zero order approximation to $F(j\omega)$.

$$\overline{F}(j\omega) = \sum_{n=-\infty}^{\infty} f(nT)e^{-j\omega nT} \qquad (3.2)$$

The zero order approximation in equation 3.2 has been divided by T to give $\overline{F}(j\omega)$, since the differential dt becomes T in the integral approximation and t has been replaced by nT in the summation, where n is any integer and T is the sampling interval. Normally, f(nT) is written as f_n, the nth sample point. $\overline{F}(j\omega)$, the discrete Fourier transform, is periodic with period $2\pi/T$. Since there are only a finite number of sample values available, the DFT must be computed over the finite sum in equation 3.3:

$$\overline{F}(j\omega) = \sum_{n=0}^{N-1} f_n e^{-j\omega nT} \qquad (3.3)$$

where N is the number of sample points. $\overline{F}(j\omega)$ possesses N complex elements, N/2 of which are independent, and is periodic with period $2\pi/T$. This suggests computing $\overline{F}(j\omega)$ with a frequency spacing, ω:

$$\omega = \frac{2\pi m}{NT} \text{ rad/sec} \qquad m = 0, 1, \ldots, N-1 \qquad (3.4)$$

This makes the equation for computing the DFT become:

$$\overline{F}_m = \sum_{n=0}^{N-1} f_n e^{-j(2\pi nm/N)} \quad m = 0, 1, \ldots, N-1 \qquad (3.5)$$

and the inverse DFT is defined as:

$$f_n = \frac{1}{N} \sum_{m=0}^{N-1} \overline{F}_m e^{j(2\pi nm/N)} \quad n = 0, 1, \ldots, N-1 \qquad (3.6)$$

Finally, the amplitude spectrum $|\overline{F}_m|$ may be obtained from the quadrature of the real and imaginary parts of $\overline{F}_m$ as shown below.

$$\overline{F}_m = \sum_{n=0}^{N-1} f_n \cos 2\pi nm/N - j \sum_{n=0}^{N-1} f_n \sin 2\pi nm/N \qquad (3.7)$$

$$\overline{F}_m = R_m + jI_m \qquad (3.8)$$

$$|\overline{F}_m| = [R_m^2 + I_m^2]^{1/2} \qquad (3.9)$$

The phase may be evaluated as:

$$\Phi = \tan^{-1}[I_m/R_m] \qquad (3.10)$$

As mentioned previously, the waveform must be sampled at a rate no less than twice the highest frequency domponent in the waveform or aliasing will result. This is

because, given a sampling interval of T seconds, the sample values at frequency v and frequency $v + nT$ are samples of a waveform with the same frequency v. Figure 17 shows the ambiguity which results if the waveform is sampled at less than twice the highest frequency. The waveform f(t) was sampled at a rate greater than twice its highest frequency, but g(t) was sampled at less than twice its highest frequency. As shown in the figure, it is possible for the two waveforms to possess the same sample set for a given T. The criterion of sampling at a rate greater than twice the highest frequency is called the Nyquist criterion. The presence of frequency components above the Nyquist frequency or sampling slower than the Nyquist criterion allows, has an effect on the DFT as shown in Figure 18c. The figure shows how aliased and shifted spectra are added to the true spectrum to form an aliased version of the DFT. The true $F(j\omega)$ and $\overline{F}(j\omega)$ are shown in Figures 18a and 18b respectively. The ultrasonic waveform should be band-limited and sampled at twice the highest frequency component. This can be accomplished by passing the signal through a low pass filter with a sharp cutoff frequency and then sampling at twice the cutoff frequency. The examples contained in this report have been sampled at 20 MHz after first

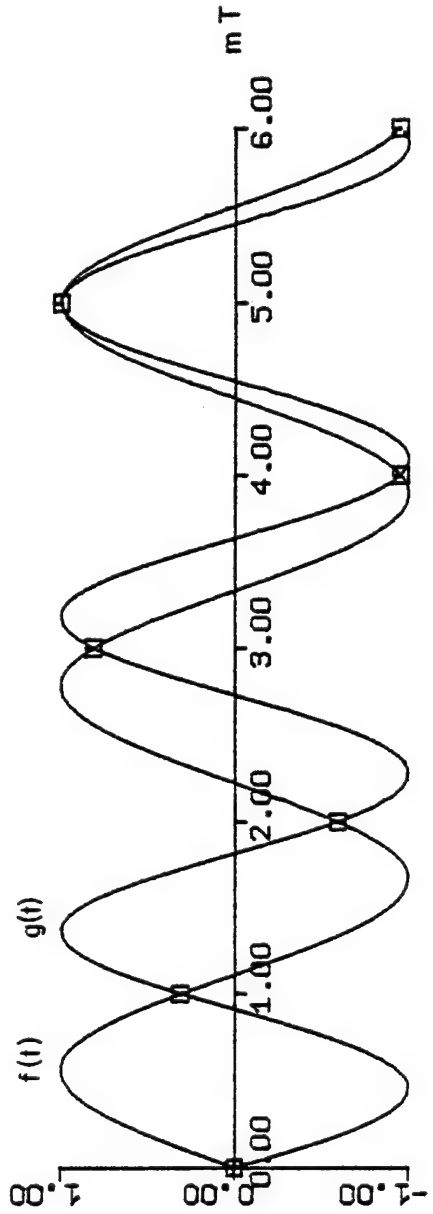

Figure 17. Sampling at Less Than the Nyquist Frequency

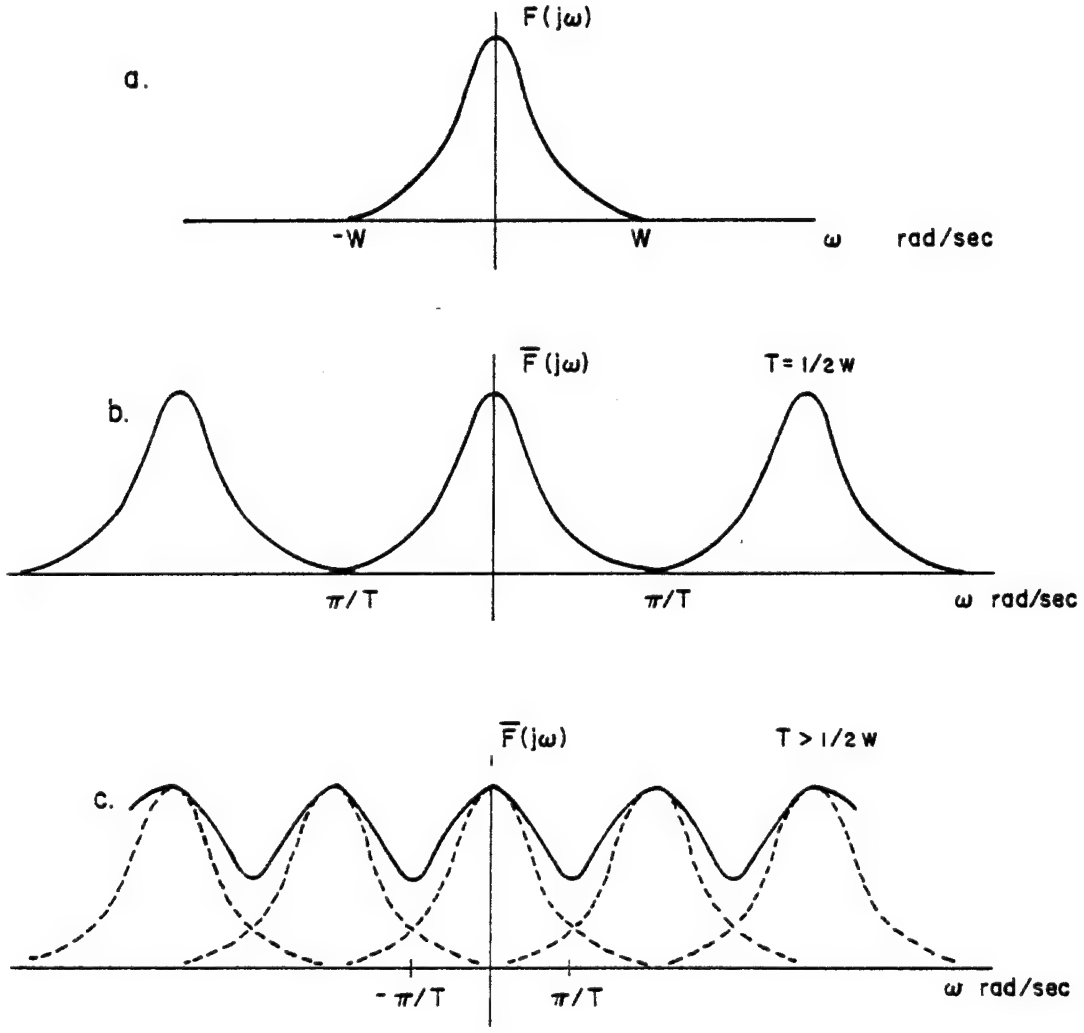

Figure 18. Aliasing in DFT

passing the signals through a fourth order Butterworth low pass filter with a 3 dB point of 10 MHz and a drop of 65 dB at 11 MHz. The computation time can be reduced substantially by the use of a fast Fourier transform algorithm, FFT. The FFT reduces the computation time by making use of the redundancy in the DFT. The DFT in equation 3.5 requires $(N)^2$ complex products to transform N sample values into N frequency values. If we define a term W_N as in equation 3.11 below,

$$W_N = e^{-j(2\pi/N)} \tag{3.11}$$

equation 3.5 reduces to equation 3.12:

$$\overline{F}_m = \sum_{n=0}^{N-1} W_N^{mn} f_n \tag{3.12}$$

We may now separate equation 3.12 into its even and odd components as shown below.

$$\overline{F}_m = \sum_{n\ even} f_n W_N^{mn} + \sum_{n\ odd} f_n W_N^{mn} \tag{3.13}$$

Substituting $n = 2\ell$ into the first sum and $n = 2\ell + 1$ into the second sum, equation 3.13 becomes:

$$\overline{F}_m = \sum_{\ell=0}^{N/2-1} f_{2\ell} W_N^{2m\ell} + \sum_{\ell=0}^{N/2-1} f_{(2\ell+1)} W_N^{(2\ell+1)m} \tag{3.14}$$

If we rewrite W_N^2 as follows:

$$W_N^2 = e^{-j2\pi 2/N} = e^{-j2\pi/N/2} = W_{N/2} \tag{3.15}$$

and substitute into equation 3.14, we have:

$$\overline{F}_m = \sum_{\ell=0}^{N/2-1} f_{2\ell} W_{N/2}^{\ell m} + W_N^m \sum_{\ell=0}^{N/2-1} f_{(2\ell+1)} W_{N/2}^{\ell m} \tag{3.16}$$

Each sum in equation 3.16 is now a DFT with N/2 points, implying that each sum requires $(N/2)^2$ complex multiplications. There are also N complex multiplications required to multiply the W_N^m terms times the second sum. There are now a total of $N^2/2 + n = N(N/2+1)$ products compared with N^2 products in the original DFT. We now make the restriction that $N = 2^n$, where n is any integer. The simplest case of a two-point FFT is shown in Figure 19. The structure shown in the figure is called a butterfly, and it is the smallest structure into which a FFT can be reduced. The numbers appearing in the butterfly are the powers of the W_N^m terms. Figure 20 shows this scheme extended to an eight-point FFT. Note that the eight-point FFT can be decomposed into two four-point FFT's. This results in the number of complex products being reduced from the original N^2 products to $(N/2)\log_2 N$ products. This becomes very important for large n. For example,

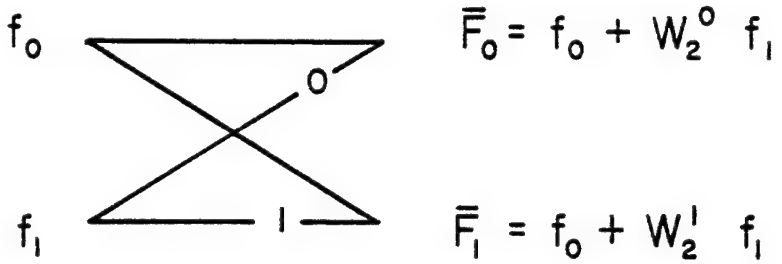

Figure 19. Two-Point FFT

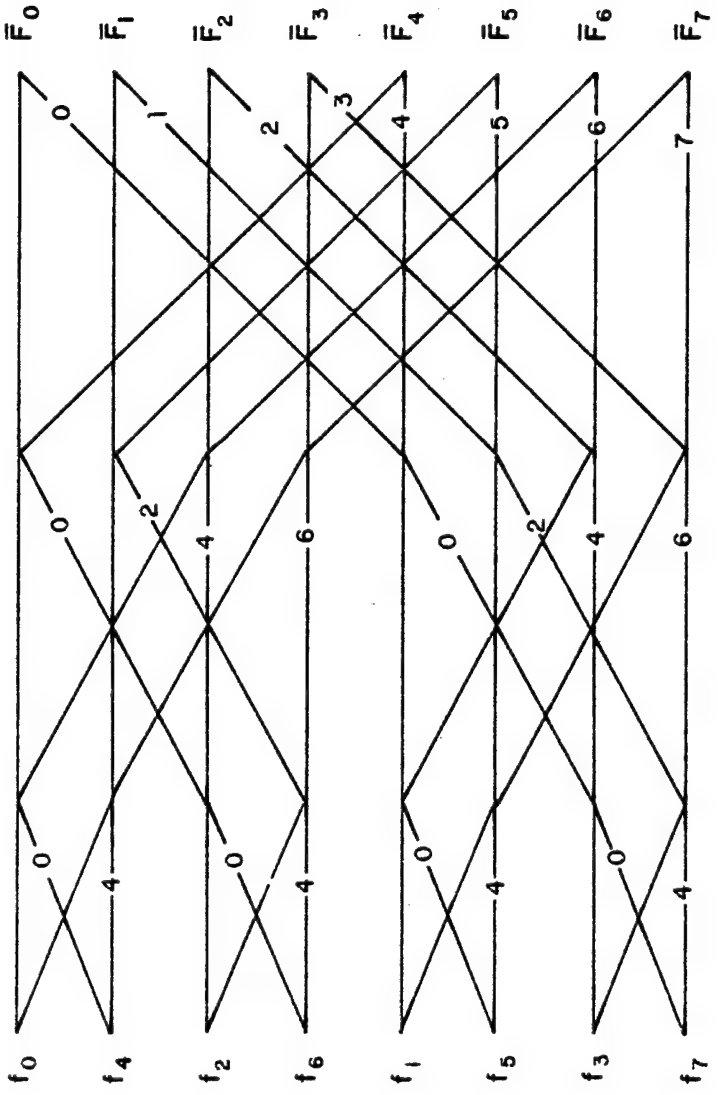

Figure 20. Eight-Point FFT

if $N = 1,024 = 2^{10}$, the number of complex products is reduced from $N^2 = 1,048,576$ to $N/2\log_2 N = 3,549$.

There are three important factors which must be considered when evaluating the results of the FFT computation. These factors are discussed in the following subsections and are shown graphically in figures.

3.2 Effect of Increasing the Number of Points in the FFT

The ultrasonic waveform is only available for a short period of time, approximately four microseconds (depending on the speed of sound through the material and the material thickness), and the sampling device has a maximum sampling rate limit. Therefore, if the sampling rate were 20 MHz, there would only be 20 samples available per microsecond of waveform. If a DFT were evaluated for these 20 samples, only 10 different frequency points in the frequency specturm would be evaluated due to the symmetry of the DFT. Thus, to obtain a good representation of the frequency spectrum between these ten points, it is necessary to "pad" the sample sequence with enough zeros to allow a continuous curve to be plotted between the original ten points. The result of padding the sample set with a different number of zeros is shown in Figures 21a and 21b.

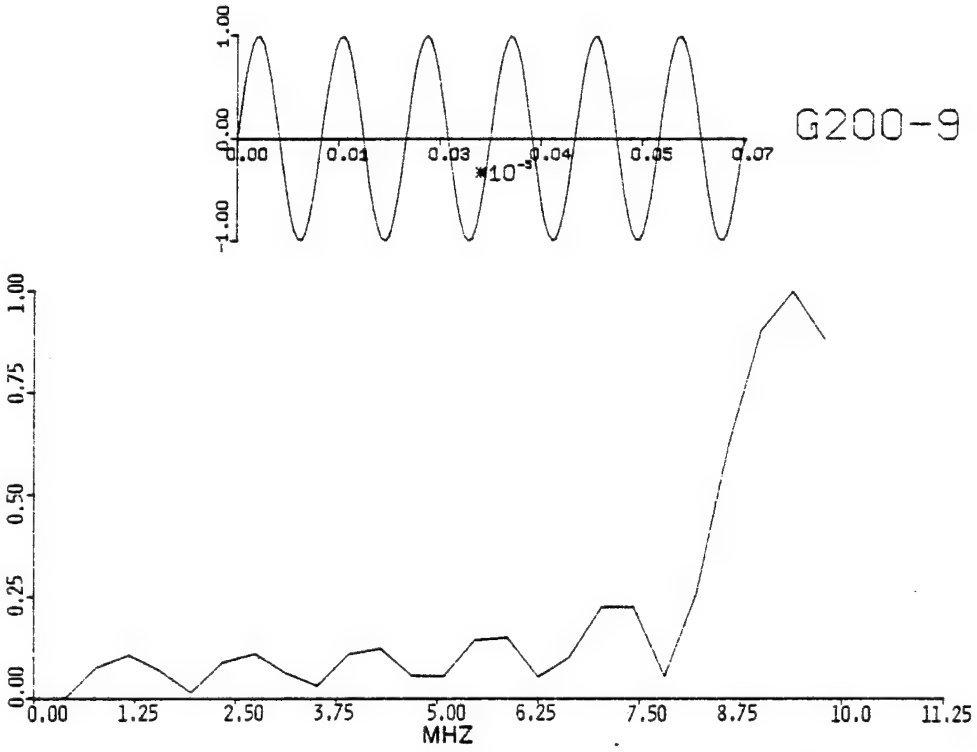

(a) 512-Point FFT of 6 Periods of 9 MHz Sine

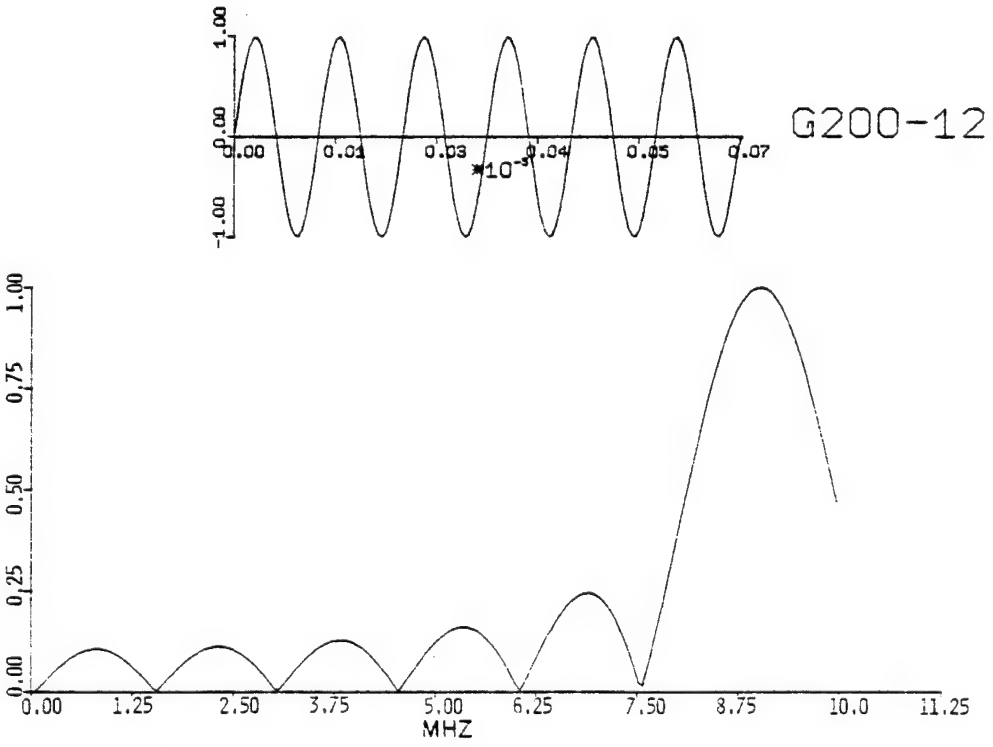

(b) 4096-Point FFT of 6 Periods of 9 MHz Sine

Figure 21

In Figure 21a, a 9 MHz sine wave was sampled at a 200 MHz rate yielding 133 sample points in six cycles of the waveform. Three hundred seventy-nine (379) zeros were added to the 133 sample points to give $2^9 = 512$ points in the FFT calculation. The frequency spacing of the resulting 256 different points allows the spectrum to be plotted up to 200 MHz, which is half the sampling rate. The first 10 MHz of the total spectrum is plotted in Figure 21a. There are only 25 points in this 10 MHz region because there are only a total of 256 points for the entire 100 MHz span of the total spectrum. If more zeros are added to the sample set to obtain $2^{12} = 4,096$ points in the FFT, the spectrum is evaluated at a much finer frequency spacing, as shown in Figure 21b. There are now 204 points plotted in the spectrum instead of 25.

3.3 Quantization Effect

The sample device is digital, which implies that the sample values are quantized and can only take on certain values. The number of different values depends on the number of quantization levels. Figures 22a through 22h show the effect of quantization of the FFT. The number appearing in the upper right corner of each figure is the number of quantization levels between -1.00 and 1.00 .

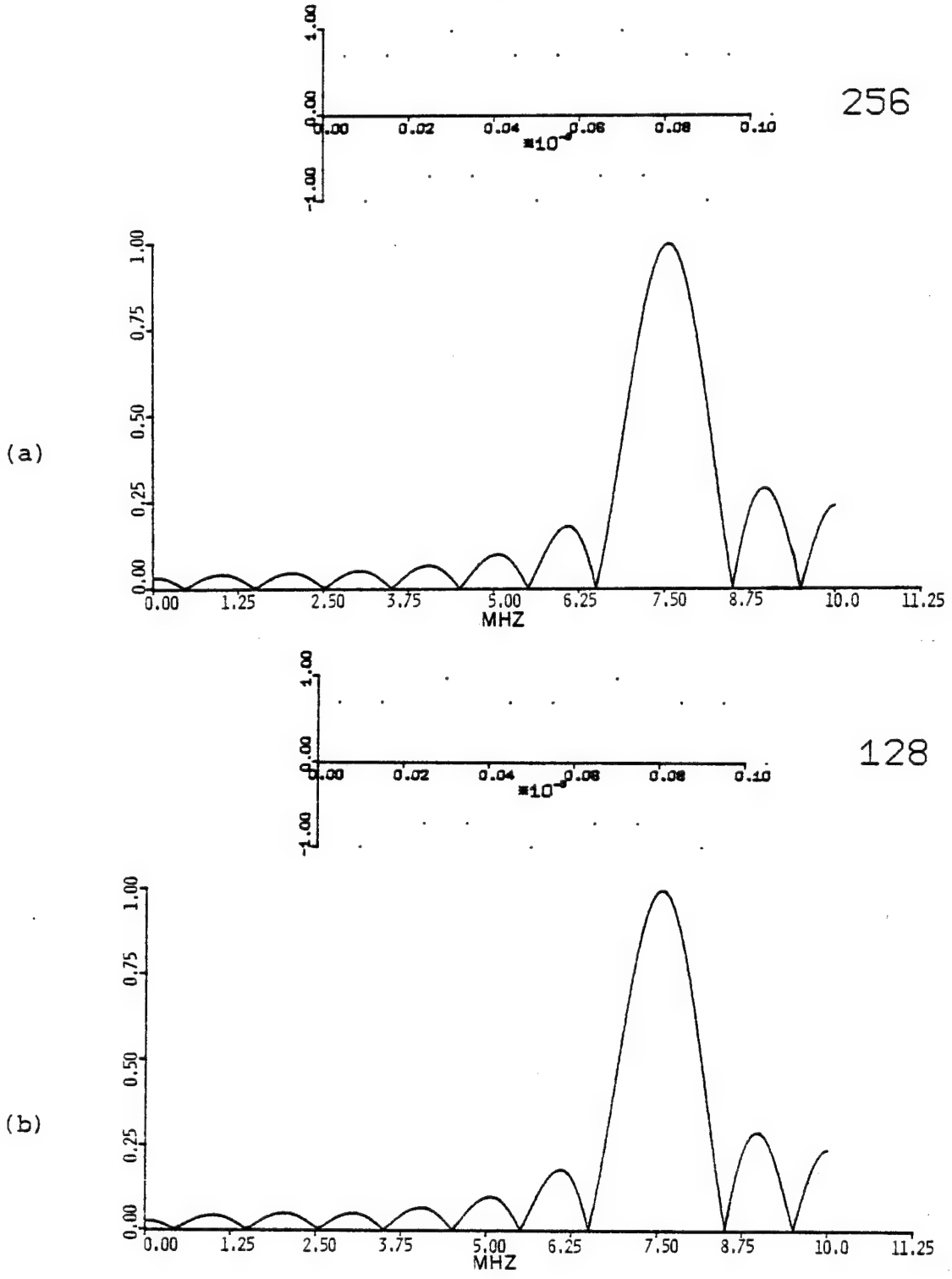

Figure 22. Quantization Effect

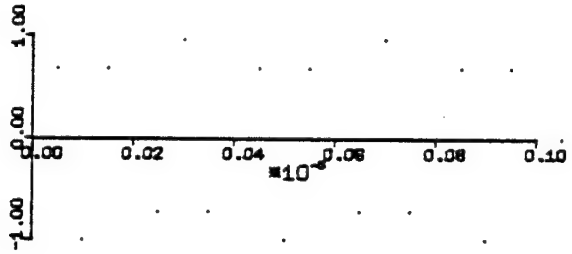

64

(c)

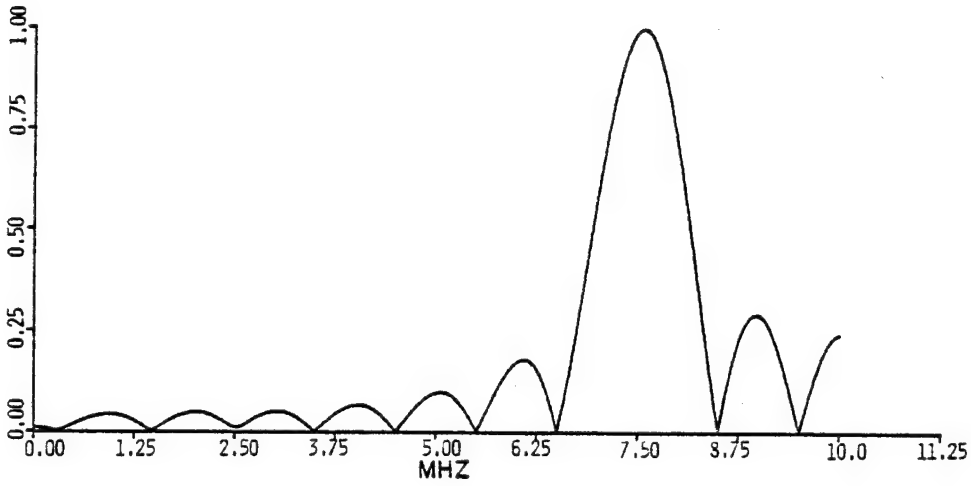

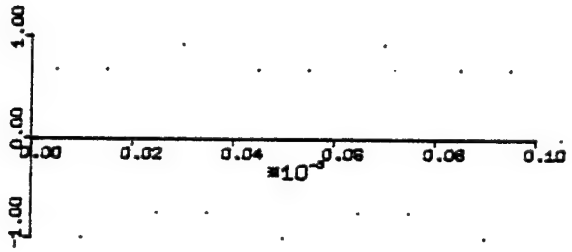

32

(d)

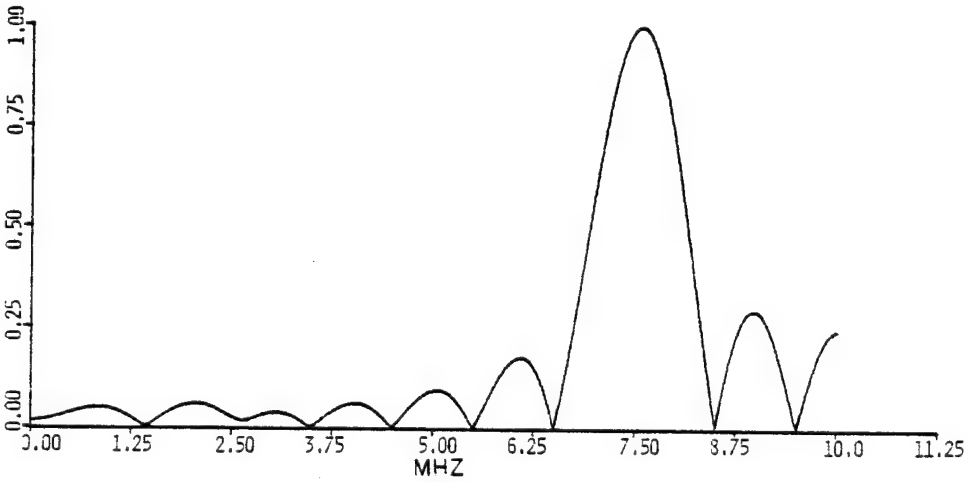

Figure 22. Quantization Effect (continued)

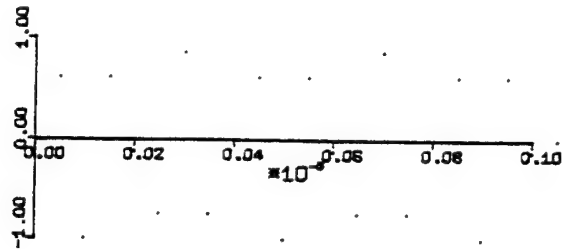

16

(e)

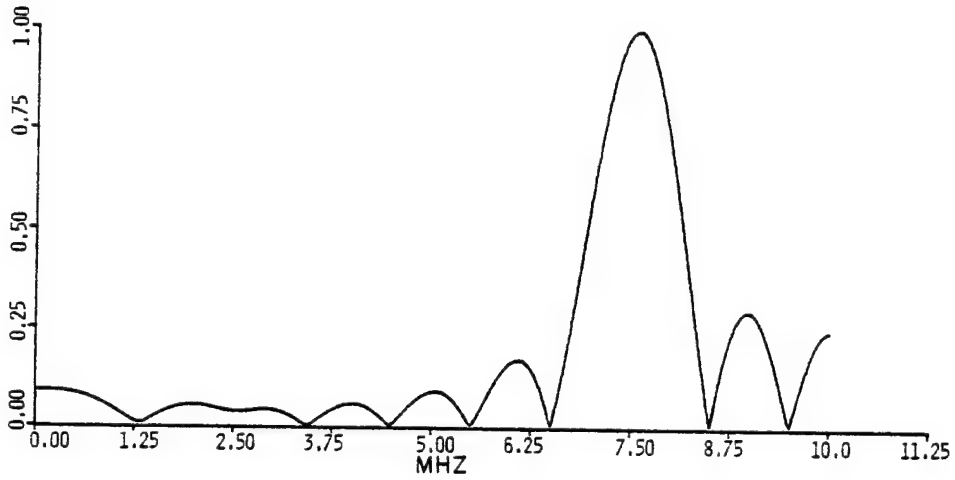

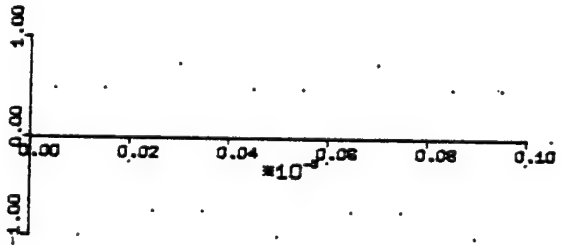

8

(f)

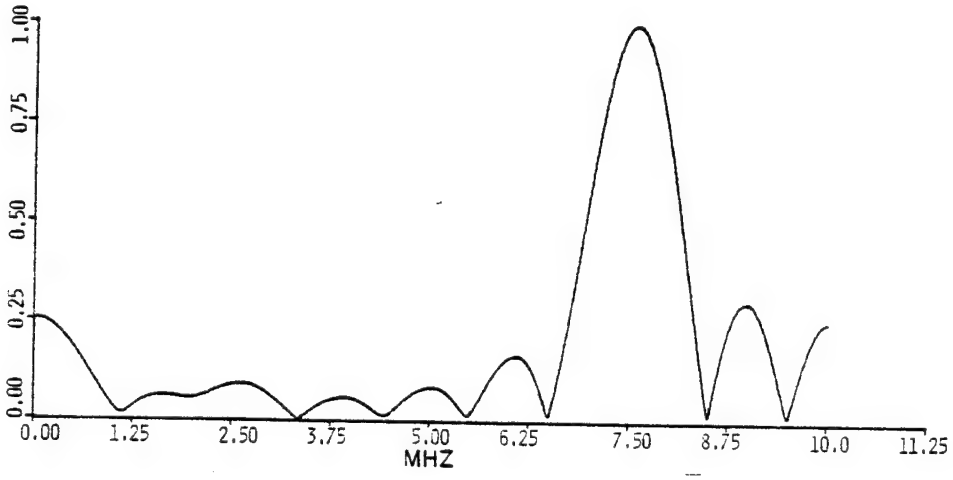

Figure 22. Quantization Effect (continued)

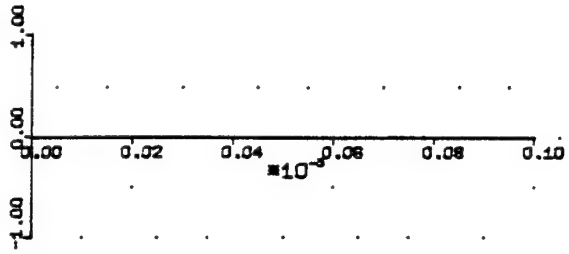

4

(g)

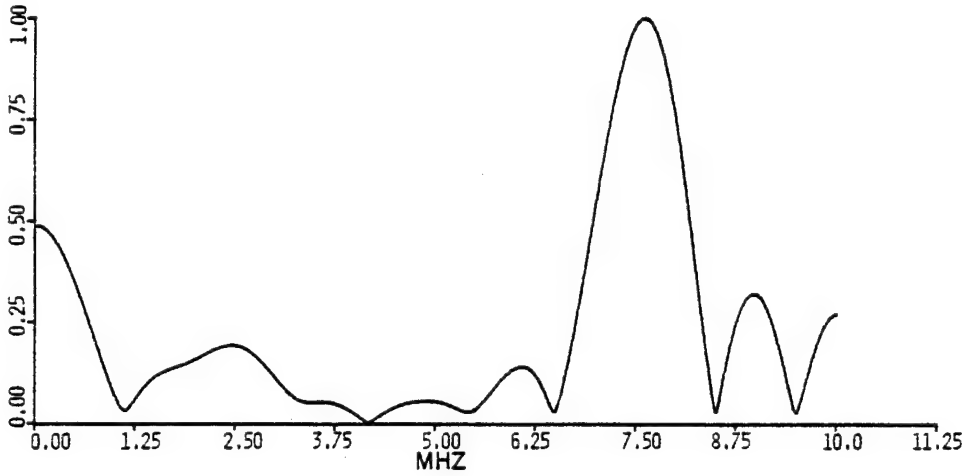

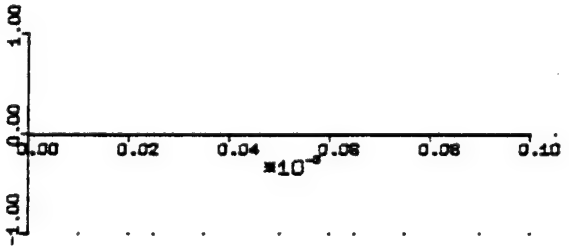

2

(h)

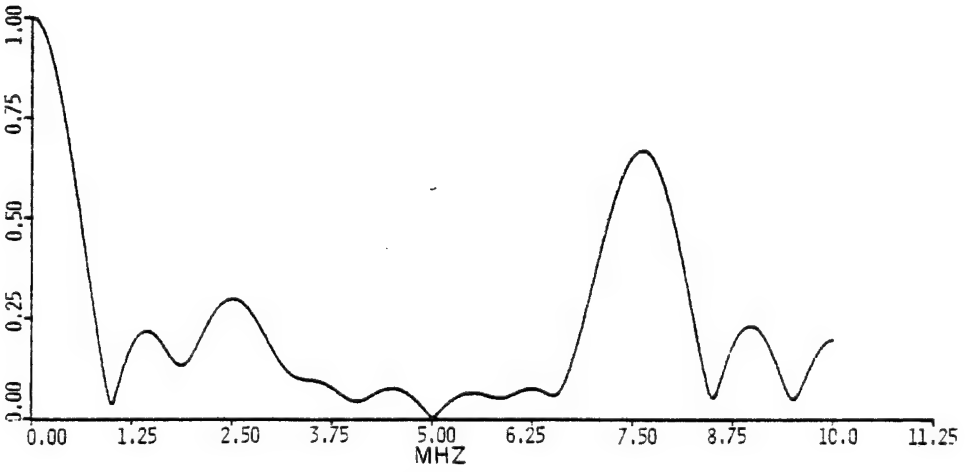

Figure 22. Quantization Effect (continued)

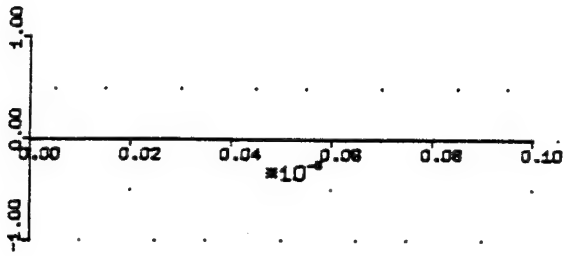

4

(g)

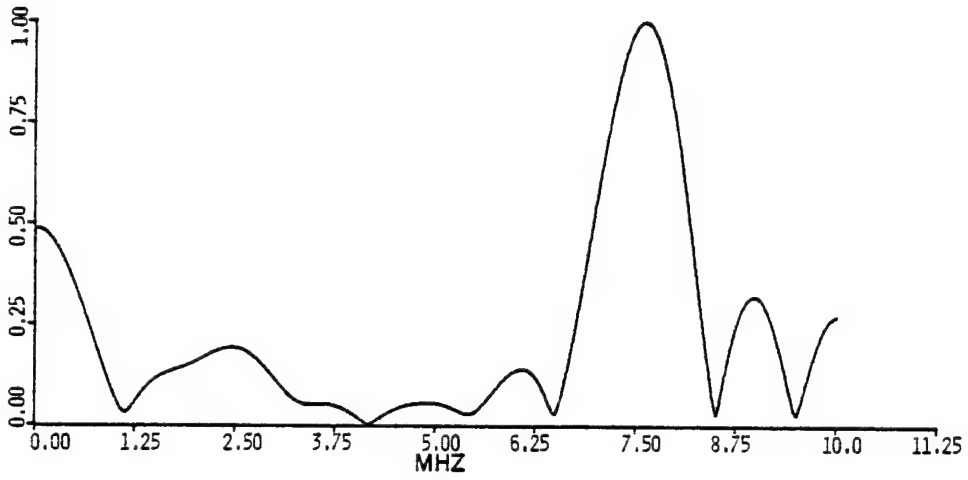

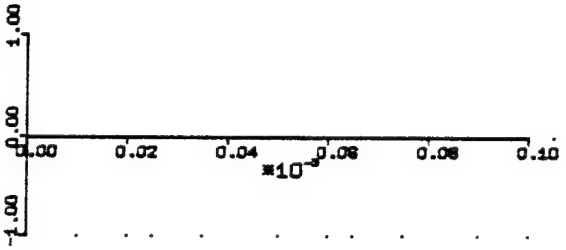

2

(h)

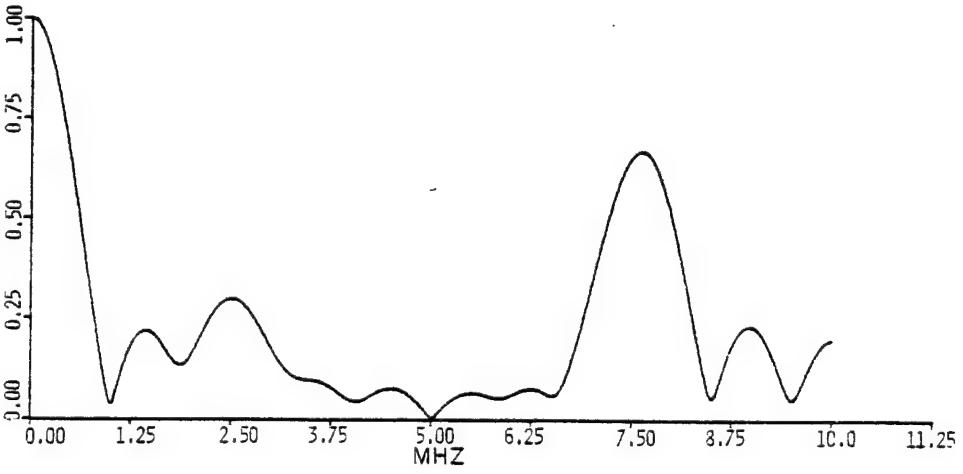

Figure 22. Quantization Effect (continued)

The dots in the top graph in each figure are the quantized sample points of a 7.5 MHz sine wave sampled at a rate of 20 MHz. Very slight differences in the resulting spectra are seen as the number of quantization levels decreases from 256 to 64; however, as the number of levels decreases from 32 to 2 a definite increase in the D.C., zero-frequency component of the spectrum is seen. The side lobes of the FFT also become distorted as the number of quantization intervals decreases. It is interesting to note that even with two quantization levels, the 7.5 MHz peak can be easily detected.

3.4 Sample Duration Effect

If the signal can be sampled for a length of time which is long compared to the period of the signal, a spectrum with sharp peaks can be produced. The size of the side lobes in the FFT will also decrease in amplitude. These effects are shown in Figures 23a through 23d, in which the number of periods of a 5 MHz sine wave is increased from 1 to 4. As the waveform is sampled for a greater number of periods, the peak in the spectrum converges and becomes sharp around the correct value. This effect is the same for both analog and digital computations and is due totally to finite signal duration.

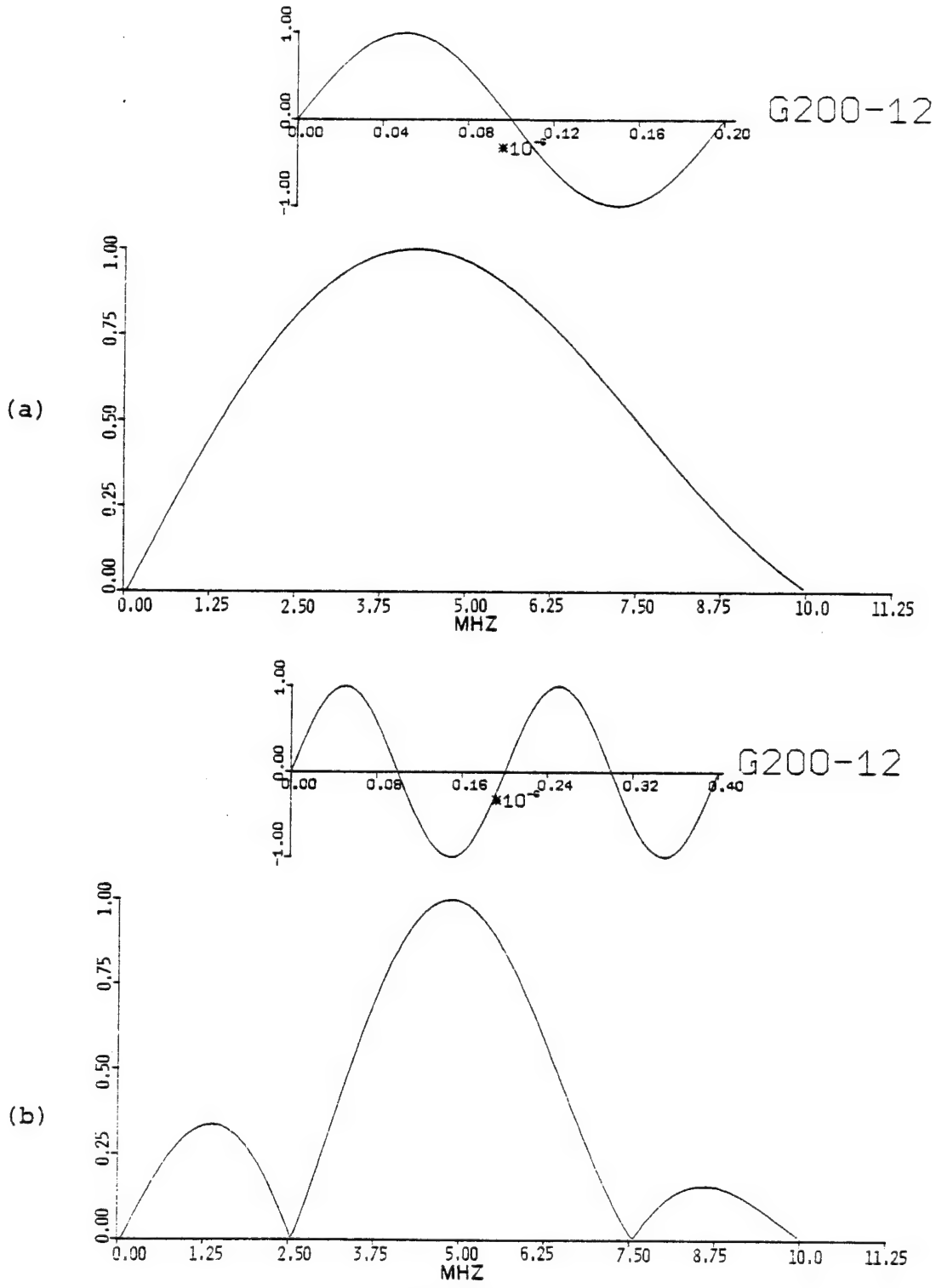

Figure 23. Sampling Duration Effect

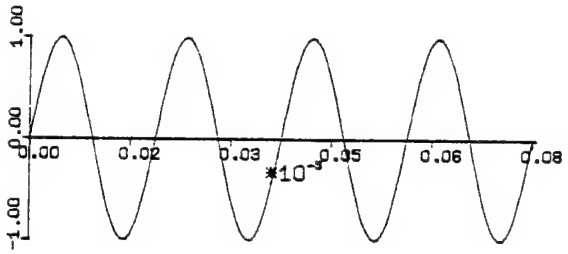

(c)

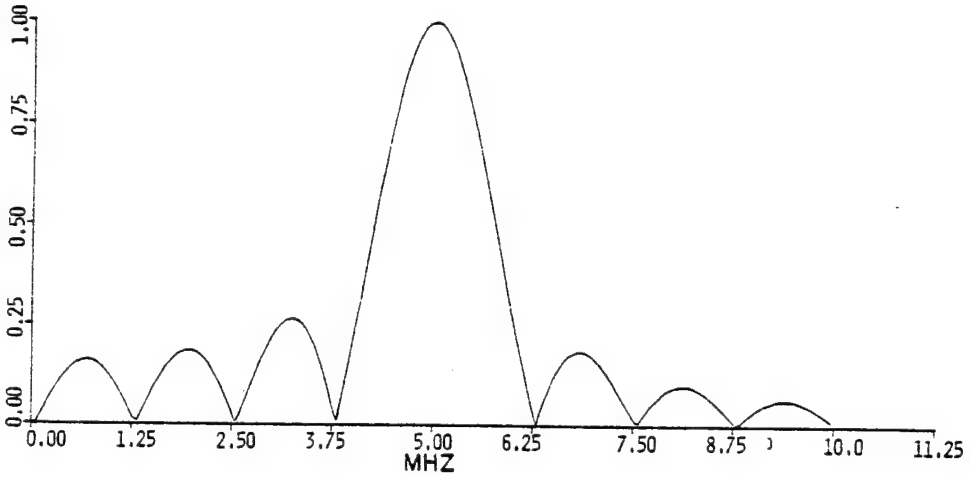

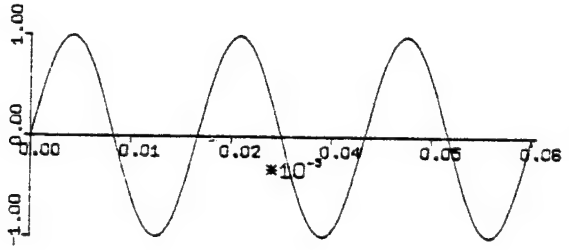

(d)

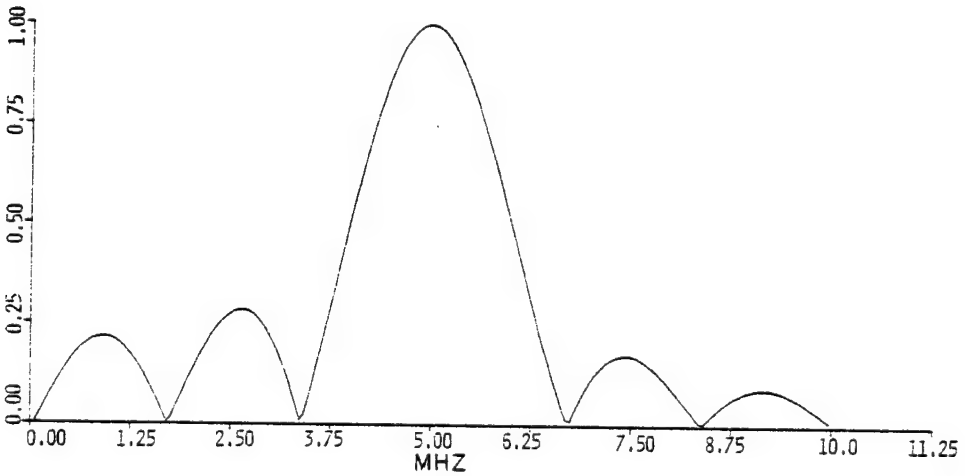

Figure 23. Sampling Duration Effect (continued)

IV. APPLICATIONS OF FREQUENCY DOMAIN TECHNIQUES

4.1 Measurement of Source Spectrum

One application of frequency domain techniques was demonstrated in Section 2.2 for the interpolation of digital A-scans. This technique required the evaluation of the frequency spectrum of the ultrasonic waveform. A program was written in Fortran IV which was capable of using the data file produced by the NICDAT program in the LSI II minicomputer. The program performs a fast Fourier transform on the ultrasonic data and produces a graphic output of the resulting frequency spectrum. In order to test the system and software with known data, a 5 MHz sine wave was generated from a function generator and input to the oscilloscope through the 10 MHz low pass filter. The input data is plotted at the top of Figure 24 and the output from the FFT program is graphed at the bottom of the figure. The deviation from 5 MHz in the frequency spectrum was found to be due to inaccuracy in the waveform generator calibration. Since the test waveform was successfully evaluated, an ultrasonic waveform from a 64-ply graphite-epoxy laminate was input into the system. The time

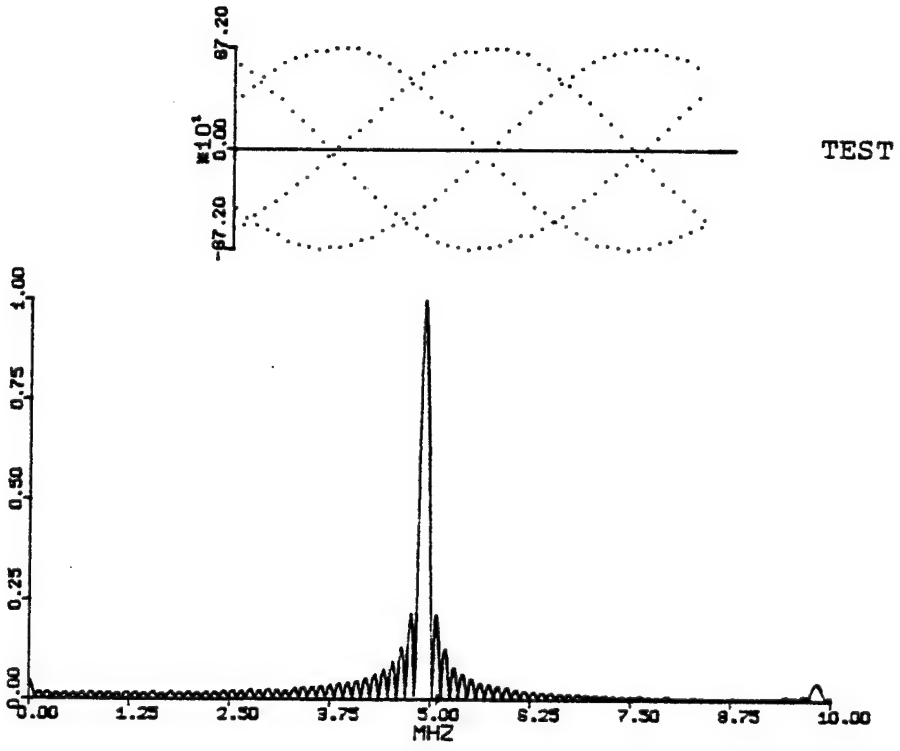

Figure 24. Test Spectrum

and frequency domain representations of the waveform are shown in Figure 25. The oscillations in the frequency spectrum, Δf , occur at regular intervals and can be related to the speed of sound c and the thickness d by the relation:

$$\Delta f = c/2d \tag{4.1}$$

The occurrence of a defect or discontinuity in the material will cause a corresponding change in the frequency spectrum. A Teflon defect was implanted between the center plies of a 64-ply graphite-epoxy laminate. An ultrasonic waveform from the defective region was input into the Fourier transform algorithm and the output is shown graphically in Figure 26. The presence of the defect between the center plies of the laminate results in the apparent thickness of the laminate to be half of the true thickness. This results in a frequency spacing Δf of twice the value of Δf when a defect was not present.

The waveforms under investigation have frequency components up to 20 MHz and, as mentioned previously, all signals are prefiltered such that they become band-limited to 10 MHz to prevent aliasing. A method was devised to retrieve the frequency components up to 20 MHz without increasing the sampling rate and is diagrammed in Figure 27.

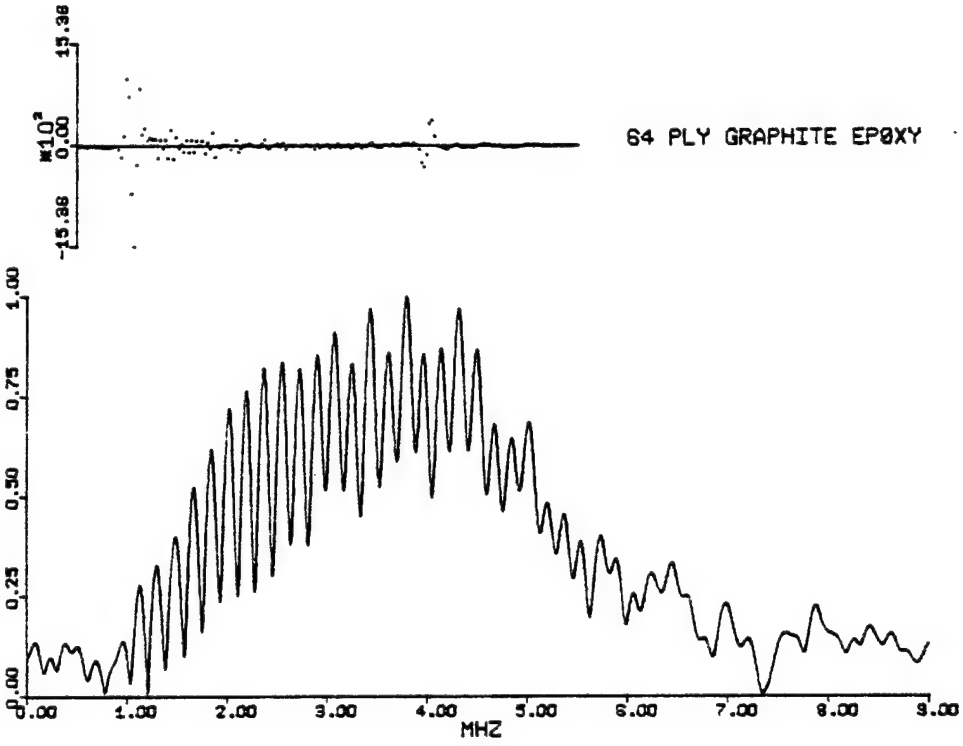

Figure 25. 64-Ply Graphite-Epoxy

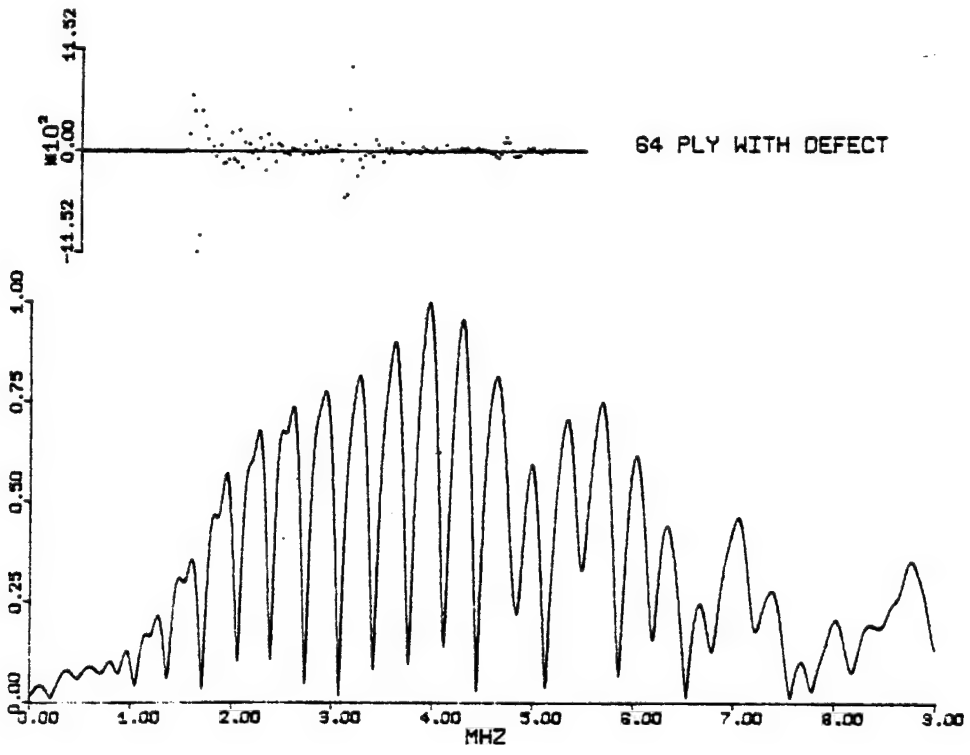

Figure 26. 64-Ply Graphite-Epoxy with Defect

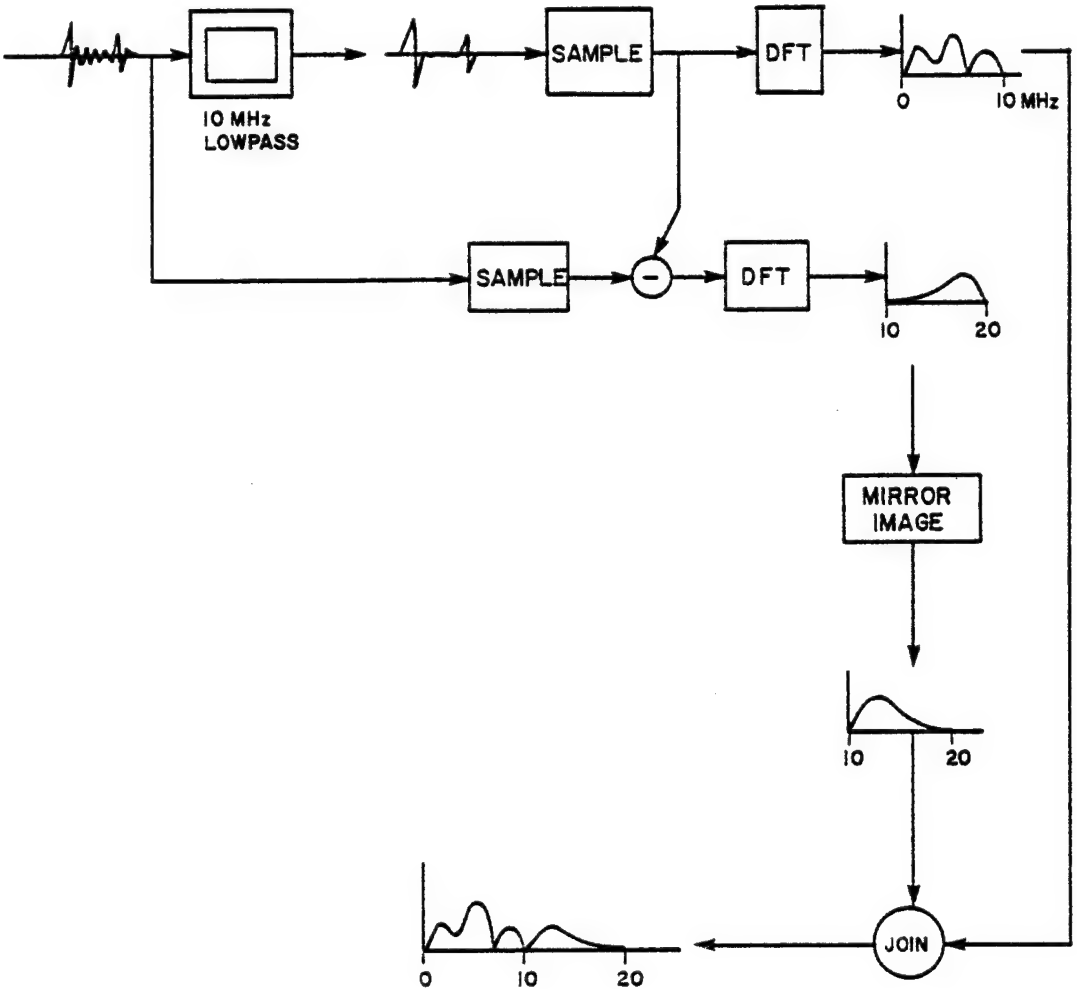

Figure 27. Two-Step Spectrum Analysis

The spectral analysis is performed in two parts. First the waveform is low-pass filtered, with zero phase shift, to 10 MHz and the Fourier transform evaluated. The 10 MHz band-limited waveform is then subtracted from the total unfiltered waveform, resulting in a waveform whose frequency components are between 10 MHz and 20 MHz. The Fourier transform of this waveform is then evaluated and its mirror image added to the end of the first transform. This results in a total frequency spectrum between 0 and 20 MHz using a two-step process which incorporated both analog and digital techniques. The mirror image of the second Fourier transform must be taken due to folding which occurs about the Nyquist frequency. This process may be continued to obtain spectra containing higher frequency components with the limiting factors of computation time and the frequency response of the sampling device.

In order to test this two-step frequency spectrum algorithm, two sine waves of different frequencies were added and used as input for the algorithm. The frequencies of the sine waves were 2.5 MHz and 15 MHz and the filtered and unfiltered sampled waveforms are plotted in the upper left and right graphs, respectively, of Figure 28. The output from the two-step frequency spectrum algorithm is shown at the bottom of the figure. The source spectrum of

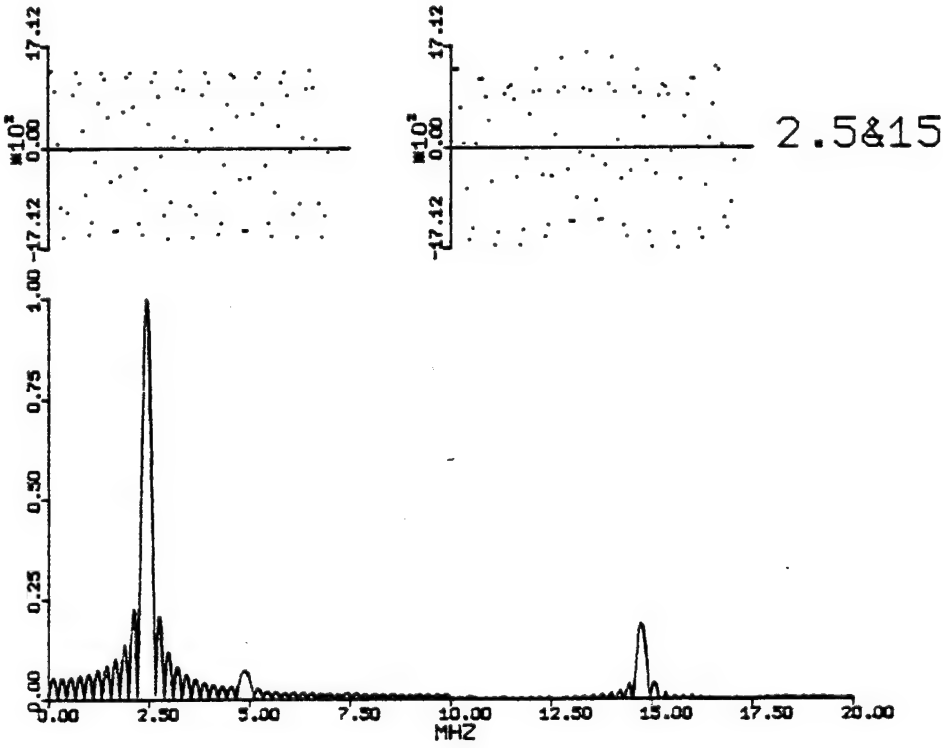

Figure 28. 2.5 and 15 MHz Test Spectrum

a 15 MHz transducer was evaluated using the above method and the graphic output is shown in Figure 29. The results correspond well with those obtained from an analog spectrum analyzer in that there is a large low frequency peak at 4 MHz and a lower amplitude peak near 15 MHz. The most significant result shown in Figure 29 is that the slope of the curve is continuous at the 10 MHz folding frequency which also tends to prove the validity of the algorithm.

4.2 Thickness Measurement by Spectral Division to Enhance Echo Peak

As previously indicated, the fluctuations in the amplitude spectrum of an ultrasonic waveform are proportional to the speed of sound and thickness of the material. This point can be exploited to form a computational tool which is capable of yielding thickness information at a position on a sample which is inaccessible by mechanical thickness measurement devices. The method of performing this measurement is to take the Fourier transform of the total ultrasonic waveform and then to take the Fourier transform of the initial pulse. This results in one spectrum which is dependent upon the material being interrogated and one spectrum which is the transducer's frequency response. The deconvolution of the two waveforms is then performed by the complex division of the two spectra.

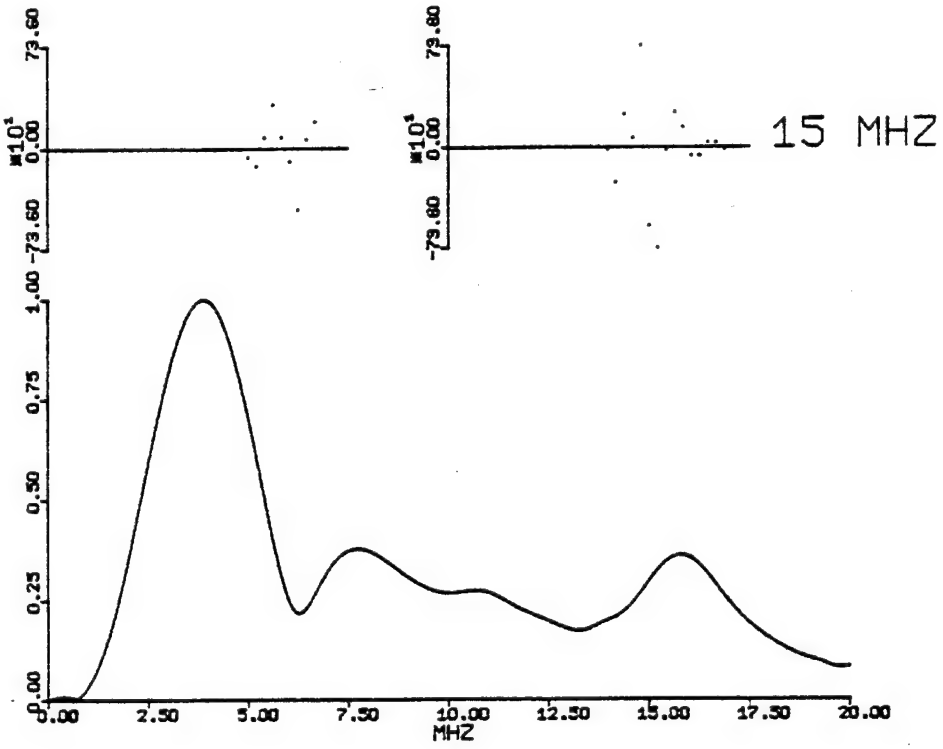

Figure 29. 15 MHz Transducer Spectrum

The data is fitted to a straight line by the least squares method. Then this line is subtracted from the data to eliminate the trend. This is necessary becasue a D.C. bias term would otherwise result in the next step of the calculation. The final step is to inverse Fourier transform the result of the complex division. This results in a time domain output which has a large peak at a given distance from the origin which corresponds to the thickness of the material at the interrogation site. An example of this technique is shown graphically in Figure 30. The time domain A-scan is graphed at the upper left of the figure and the result of the complex division and least square fit is displayed at the upper right of the figure. The result of the final Fourier transform is shown at the bottom of Figure 30. The scale at the bottom of the figure can be calibrated for the units of measure desired, knowing the speed of sound in the material, or it can be used as an indicator of defect location. This aspect of the technique is demonstrated in Figure 31 which applies the above method to a 64-ply graphite-epoxy sample with an implanted defect between its center plies. It can be seen that the distance of the echo peak from the origin has been halved and thus indicates a center ply defect.

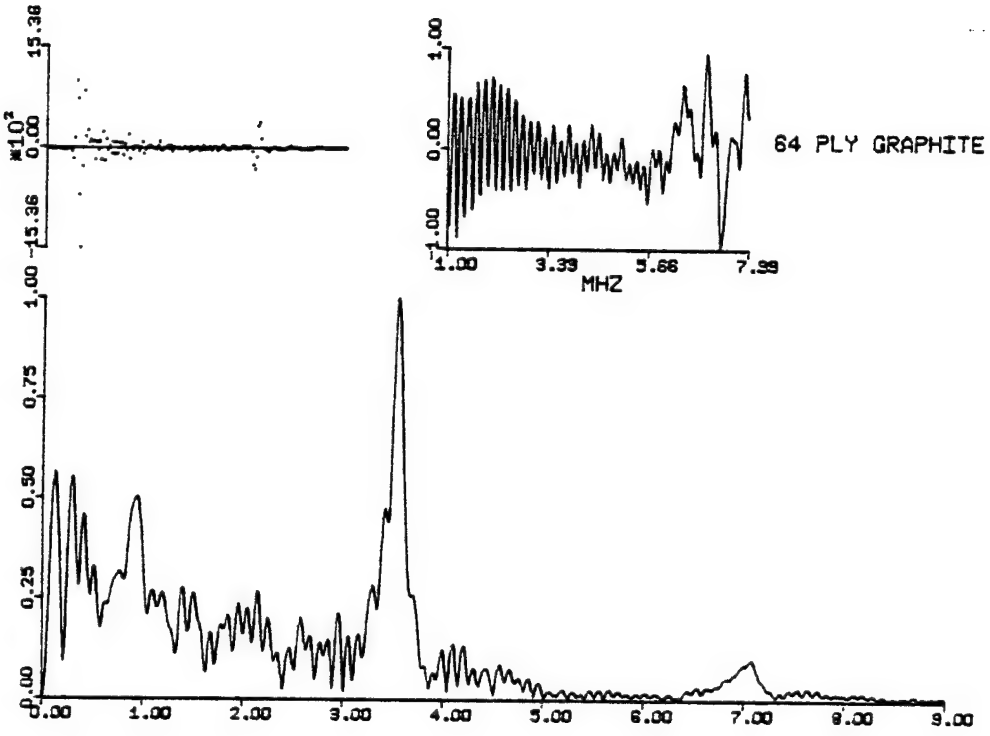

Figure 30. Echo Peak Enhancement for 64-Ply Graphite-Epoxy

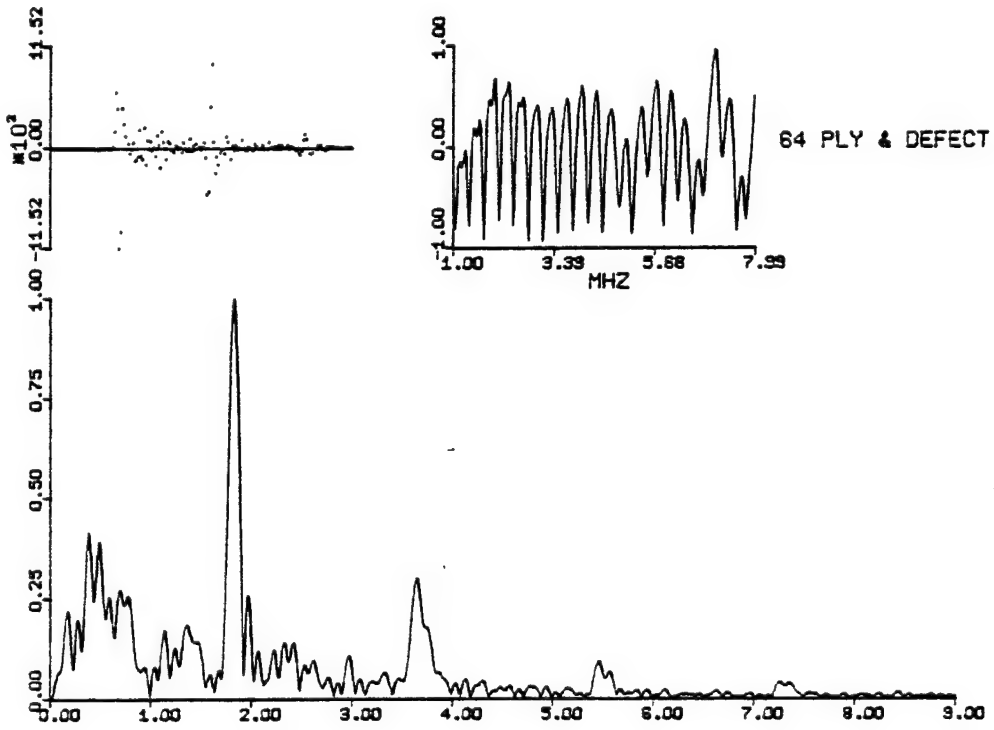

Figure 31. Echo Peak Enhancement for 64-Ply Graphite-Epoxy with Defect

4.3 Velocity of Sound Measurement by Phase Angle Computation

The method described in the previous subsection requires and accurate measurement of the velocity of sound in the sample. The velocity of sound measurement could be made from the time domain representation of the waveform except that the points at which the measurements should be made are not well defined. The measurement could also be made from the Δf measurement in the frequency spectrum of the material except that this gives a discrete number of velocity measurements averaged over various frequency bands. A more accurate and continuous measurement of velocity of sound as a function of frequency can be obtained from measurements of the phase of the front surface echo and back surface echo independently. The phase of the two echos can be determined from the Fourier transform of the individual echos, and the graphic representation of this phase information for a 1/4" Plexiglas sample is given in Figure 32. The vertical lines in the time representation of the waveform indicate the regions over which the phase information is calculated for each echo. The first two vertical lines are the boundaries for the front surface echo and the second two lines are the boundaries for the

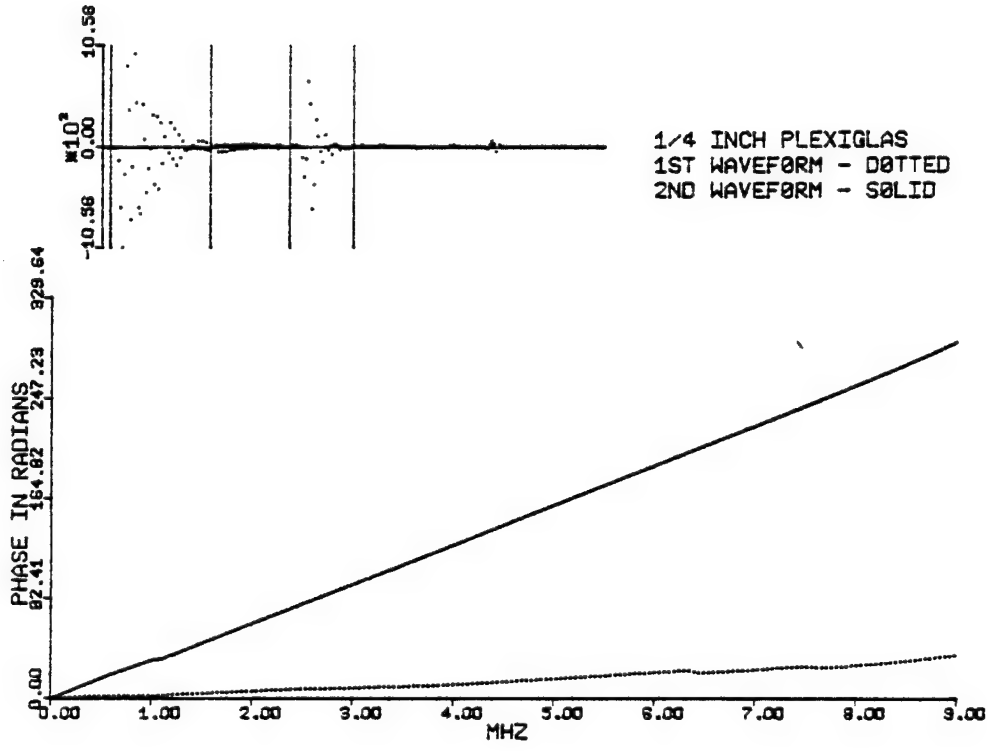

Figure 32. Phase Angle Data for 1/4" Plexiglas

back surface echo. This phase information can be used to determine the velocity of sound in the sample as a function of frequency, and the theory behind the measurement is diagrammed in Figure 33. A phase measurement is made at the first surface ϕ_0 and at the second surface ϕ_1. The thickness of the sample must be measured at the point on the sample where the phase measurements are made. With this information the velocity of sound can be evaluated using equation 4.2 .

$$c(\omega) = \frac{2d\omega}{[\phi_1(\omega) - \phi_0(\omega)]} \qquad (4.2)$$

The results of this computation are shown for a 1/4" Plexiglas sample in Figure 34 and for a 1/4" graphite-epoxy sample in Figure 35. The vertical lines in the waveforms at the top of the figures indicate the boundaries for which the phase measurements were evaluated.

The velocity of sound measurement can also be of importance in the evaluation of material elastic constants. The speed of sound propagating normal to the surface of a composite material is a function of the elastic constant C_{33} according to equation 4.3 :

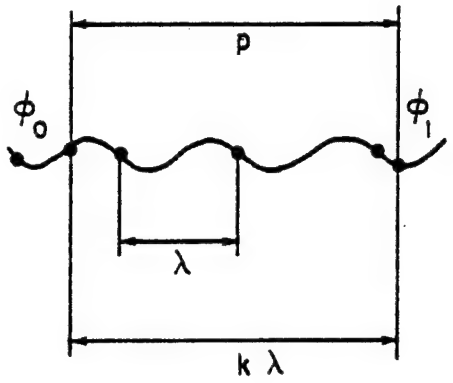

p = PATH LENGTH OF SOUND

λ = WAVE LENGTH

ϕ_0 = PHASE AT INTERFACE 0

ϕ_1 = PHASE AT INTERFACE 1

k = NUMBER OF CYCLES

c = VELOCITY OF SOUND

d = THICKNESS OF SAMPLE

f = FREQUENCY OF SOUND

ω = FREQUENCY IN RAD/SEC

$$\lambda = c/f \qquad c = \lambda f \qquad \omega = 2\pi f$$

$$(\phi_1 - \phi_0) = 2\pi k \qquad k\lambda = p \qquad p = 2d$$

$$c = \frac{p f 2\pi}{(\phi_1 - \phi_0)} = \frac{p\omega}{(\phi_1 - \phi_0)}$$

$$c(\omega) = \frac{2d\omega}{(\phi_1(\omega) - \phi_0(\omega))}$$

Figure 33. Phase Velocity of Sound

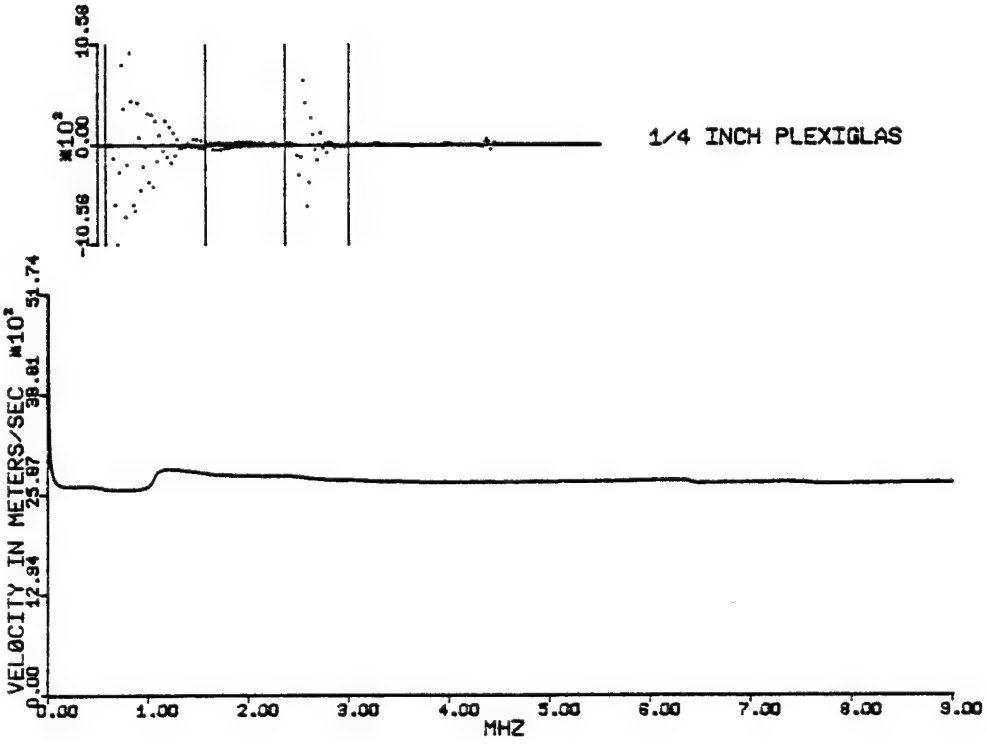

Figure 34. Velocity of Sound Measurement for 1/4" Plexiglas

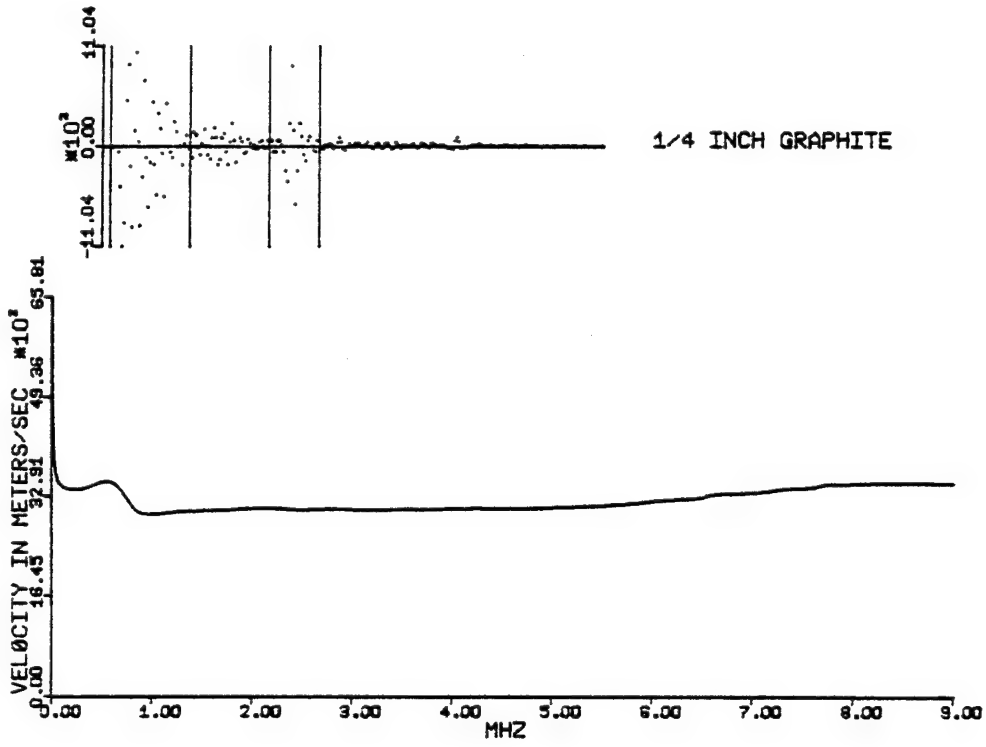

Figure 35. Velocity of Sound Measurement for 1/4" Graphite

$$c = (C_{33}/\rho)^{1/2} \tag{4.3}$$

where ρ is the density of the composite.[2]

To compare this measurement with experimental results from mechanical testing, a special sample was fabricated in which the fiber ends were normal to the incident sound beam. This will result in an elastic constant C_{11} which is easily measured in a mechanical testing lab. The results were 126 GP (Giga Pasclas) for the mechanical testing lab and 131 GP for the ultrasonic measurement. This is an experimental difference of 4% which can be explained by differences in volume fractions between specimens. It is an easy task to measure C_{33} ultrasonically; however, there is little mechanical experimental data with which to compare such measurements due to the difficulties involved with mechanical measurement. It is for this reason that the special sample was fabricated and the C_{11} measurement was performed.

---

[2]Scott. Ultrasonic Spectrum Analysis for NDT of Layered Composite Materials, Report No. NADC-75324-30, NADC, Warminster, Pennsylvania, 1975.

V. CONCLUSIONS

This report has demonstrated the capability of a digital system to perform the same functions as an equivalent analog system. It has shown that the digital system is a powerful tool, because of its versatility and ability to display results in a variety of forms. A digital system is easily adapted to performing new tasks by software modifications and seldom requires changes in hardware.

The use of frequency domain measurements rather than time domain measurements allows a better defined measurement of ultrasonic material properties to be made than is possible with time domain information alone. The report has shown applications of digital frequency domain techniques to composite material evaluation. Thickness measurements, defect locations, velocities of sound and material property determinations have all been made using frequency domain information; and in the case of material property measurement it is possible to obtain ultrasonic measurements of some properties that are very difficult to measure by mechanical test methods.

APPENDIX A.

LSI II/Nicolet Oscilloscope

Software Flow Chart

NICDAT

LOW LIMIT LOCATION 3100
HIGH LIMIT LOCATION 2160
LIMITS MUST BE ENTERED IN OCTAL

CONTROL CHARACTERS

P.....ACTIVATES OR HALTS PUNCH
B.....TRANSMITS BREAK COMMAND
G.....TRANSFERS CONTROL BETWEEN TERMINALS
N.....INITIALIZES DATA TRANSFER OPERATION.....LA36 ONLY
T.....INITIATES DATA TRANSFER.....LA36 ONLY

BREAK KEY TRANSFERS CONTROL FROM PROGRAM TO LSI II

26G RESTARTS PROGRAM

DATA IS TRANSFERED BETWEEN 48 AND 57 MICROSECONDS UNLESS LIMITS ARE CHANGED

3100/0000	AND	2160/10000	TRANSFER TOTAL WAVEFORM
3100/0000	AND	2160/4000	TRANSFER HALF WAVEFORM

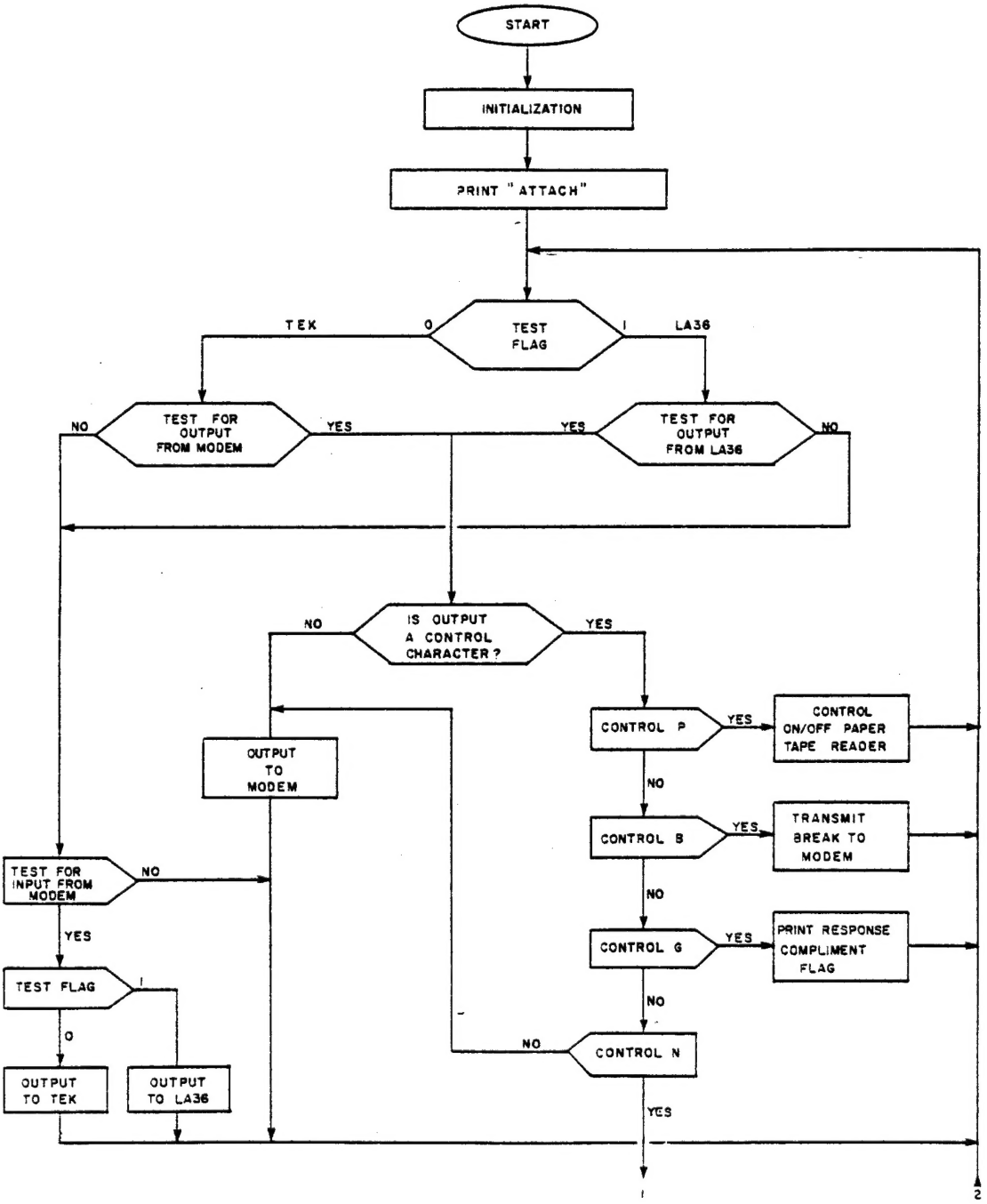
START
INITIALIZATION
PRINT " ATTACH"
TEST FLAG
0
TEK
1
LA36
TEST FOR OUTPUT FROM MODEM
NO
YES
YES
TEST FOR OUTPUT FROM LA36
NO
IS OUTPUT A CONTROL CHARACTER ?
NO
YES
OUTPUT TO MODEM
CONTROL P
YES
CONTROL ON/OFF PAPER TAPE READER
NO
CONTROL B
YES
TRANSMIT BREAK TO MODEM
NO
CONTROL G
YES
PRINT RESPONSE COMPLIMENT FLAG
NO
CONTROL N
NO
YES
TEST FOR INPUT FROM MODEM
NO
YES
TEST FLAG
1
0
OUTPUT TO TEK
OUTPUT TO LA36
1
2

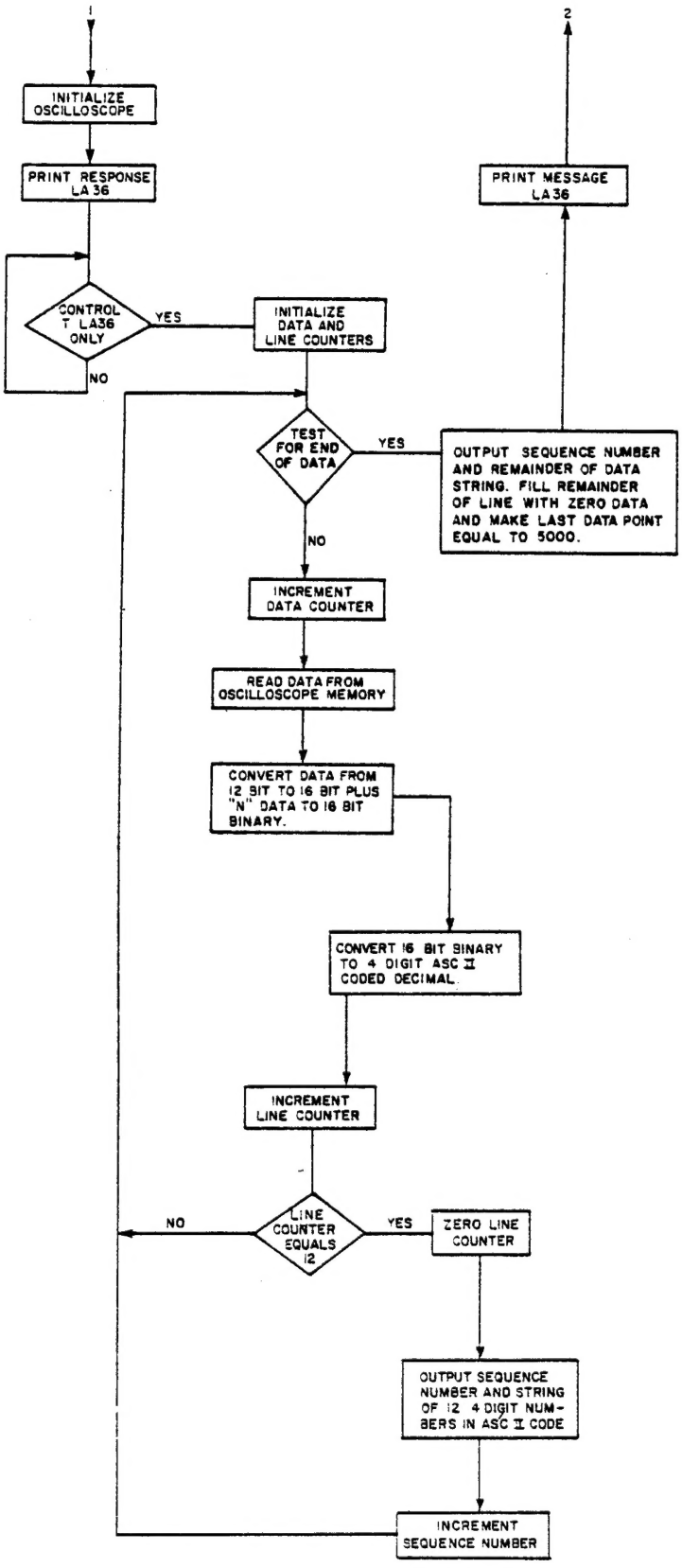
1
INITIALIZE OSCILLOSCOPE
PRINT RESPONSE LA36
CONTROL T LA36 ONLY
YES
INITIALIZE DATA AND LINE COUNTERS
NO
TEST FOR END OF DATA
YES
OUTPUT SEQUENCE NUMBER AND REMAINDER OF DATA STRING. FILL REMAINDER OF LINE WITH ZERO DATA AND MAKE LAST DATA POINT EQUAL TO 5000.
2
PRINT MESSAGE LA36
NO
INCREMENT DATA COUNTER
READ DATA FROM OSCILLOSCOPE MEMORY
CONVERT DATA FROM 12 BIT TO 16 BIT PLUS "N" DATA TO 16 BIT BINARY.
CONVERT 16 BIT BINARY TO 4 DIGIT ASC II CODED DECIMAL.
INCREMENT LINE COUNTER
LINE COUNTER EQUALS 12
NO
YES
ZERO LINE COUNTER
OUTPUT SEQUENCE NUMBER AND STRING OF 12 4 DIGIT NUMBERS IN ASC II CODE
INCREMENT SEQUENCE NUMBER